The Role of Uncertainty in Forecasting Realized Covariance of US State-Level Stock Returns: A Reverse-MIDAS Approach

Jiawen Luo*, Shengjie Fu**, Oguzhan Cepni*** and Rangan Gupta****

Abstract

In this paper, we construct a set of reverse-Mixed Data Sampling (MIDAS) models to forecast the daily realized covariance matrix of United States (US) state-level stock returns, derived from 5-minute intraday data, by incorporating the information of volatility of weekly economic condition indices, which serve as proxies for economic uncertainty. We decompose the realized covariance matrix into a diagonal variance matrix and a correlation matrix and forecasting them separately using a two-step procedure. Particularly, the realized variances are forecasted by combining Heterogeneous Autoregressive (HAR) model with the reverse-MIDAS framework, incorporating the low-frequency uncertainty variable as a predictor. While the forecasting of the correlation matrix relies on the scalar MHAR model and a new log correlation matrix parameterization of Archakov and Hansen (2021). Our empirical results demonstrate that the forecast models incorporating uncertainty associated with economic conditions outperform the benchmark model in terms of both in-sample fit and out-of-sample forecasting accuracy. Moreover, economic evaluation results suggest that portfolios based on the proposed reverse-MIDAS covariance forecast models generally achieve higher annualized returns and Sharpe ratios, as well as lower portfolio concentrations and short positions.

Keywords: US state-level stock returns; Covariance matrix; Uncertainty; Reverse-MIDAS; Forecasting

JEL Codes: C22; C32; C53; D80; G10

* School of Business Administration, South China University of Technology, Guangzhou 510640, China.Email: 2jialuo@163.com.

** School of Business Administration, South China University of Technology, Guangzhou 510640, China.Email: bm_shengjiefu@mail.scut.edu.cn.

*** Ostim Technical University, Ankara, Turkiye; University of Edinburgh Business School, Centre for Business, Climate Change, and Sustainability; Department of Economics, Copenhagen Business School, Denmark. Email address: oce.eco@cbs.dk.

**** Corresponding author. Department of Economics, University of Pretoria, Private Bag X20, Hatfield 0028, South Africa. Email address: rangan.gupta@up.ac.za.

1. Introduction

The accurate modeling and forecasting of covariance matrices plays a critical role in modern portfolio theory and risk management frameworks. Traditional approaches in the literature, such as multivariate Generalized Autoregressive Conditional Heteroskedasticity (GARCH) models (see, Bauwens et al. (2006) for a review) and Stochastic Volatility (SV) models (Harvey et al., 1994), treat the covariance matrix as a latent variable but are limited in their ability to incorporate intraday information. To address this limitation, Andersen et al. (2003) introduced the realized covariance (RCOV) matrix, which leverages on high-frequency intraday trading data to provide a model-free representation, thus reducing computational complexity. Building on this foundation, numerous studies have explored RCOV forecasting methods. Chiriac and Voev (2011) proposed the multivariate heterogeneous autoregression (MHAR) model for RCOV, an extension of the (2009) univariate HAR model of Corsi (2009) to the multivariate domain. This model is simple, straightforward to estimate using ordinary least squares (OLS), and retains the structural intuition of the original HAR model, involving long-memory and multi-scaling properties.

In this regard, Bauer and Vorkink (2011) employed the matrix-logarithm transformation to ensure positive-definite forecasts of RCOV. Oh and Patton (2016) utilized the DRD decomposition to separately model realized variances and realized correlations. Bollerslev et al. (2018) incorporated measurement errors into the scalar MHAR model and enhance the RCOV forecasting accuracy. Vassallo et al. (2021) employed the Dynamic Conditional Correlation (DCC) approach and propose a class of score-driven realized covariance forecasting models. Gribisch and Hartkopf (2023) generalized the Wishart state-space model for RCOV modeling and forecasting. Li et al. (2024) developed a robust estimation scheme for the scalar MHAR model, utilizing the multivariate least-trimmed squares method to forecast realized covariance.. Zhang et al. (2024) forecasted the realized covariance matrix of US equity returns by considering the predictive information of graphs in volatility and correlation. However, these studies utilize only the information related to the RCOV itself, such as its own lags, and often neglect the potential role of exogenous variables. While many studies on realized volatility forecasting frequently incorporate external information, with the review of this literature beyond the scope of this paper,[1] few studies extend this perspective to covariance matrix forecasting. Notable exceptions include Asai et al. (2020), who integrated geopolitical risks into the model for forecasting the realized covariances crude oil and gold futures.

Existing studies on forecasting the RCOV of stock market primarily consider a subset of stocks of the overall index (such as the Dow Jones and the S&P 500) as the sample (Callot et al., 2016; Opschoor et al., 2018; Pakel et al., 2021; Bauwens and Otranto, 2023; Alves et al., 2024; Li et al., 2024). Yet, the modeling of RCOV at the regional-level remains largely unexplored. This paper addresses this gap by forecasting the RCOV of state-level stock market indices of the US, derived from 5-minute intraday data. Importantly, it also examines whether the volatility of weekly state-level Economic Conditions Indices (ECIs), developed by Baumeister et al. (2022), provides predictive power.. Note that, the ECIs cover multiple dimensions namely, mobility measures, labor market indicators, real economic activity, expectations measures, financial indicators, and household indicators, and hence its volatility, can be considered a metric of overall macroeconomic uncertainty (Salisu et al., 2025).

At this juncture, it must be pointed out that the nexus between RCOV and uncertainty can be intuitively rationalized. First, according to the present value model of asset prices (Shiller, 1981a, b), stock market volatility depends on the variability of cash flows and the discount factor, which in turn, is driven by economic uncertainty (Bernanke, 1983; Schwert, 1989). Second, recent empirical studies by Polat et al. (2024) and Cepni et al. (2024) demonstrated strong evidence of comovement (connectedness) not only among state-level stock returns but also among ECIs.. This suggests correlations across state stock markets, on its own, and also possibly due to underlying economic conditions, given the well-established role of the business cycle in driving general stock market movements (Goyal et al., 2024). Considering the impact of

[1] A good summary is provided in Gunnarsson et al. (2024), and Luo et al. (forthcoming).

economic conditions on realized volatility and realized correlation, it is reasonable to hypothesize that first- and second-moment movements in ECIs may have predictive power for RCOV.

Econometrically speaking, to implement the mixed-frequency forecasting exercise involving daily RCOV with the volatility of weekly ECIs, we utilize the reverse-MIDAS (RM) framework of Foroni et al. (2018). Specifically, we decompose the RCOV into a realized variances matrix ($\boldsymbol{D}_t$) and a realized correlation matrix ($\boldsymbol{R}_t$) using the DRD approach and model them separately. For the realized variances ($\boldsymbol{D}_t$), we propose a class of RM-HARX models to incorporate weekly information of the second-moment of the ECIs to individually forecast the realized variances (RVs), the diagonal elements of $\boldsymbol{D}_t$. Particularly, these models are built on the HAR model (Corsi, 2009) and the RM framework. The former characterizes the long memory of RV, as documented by Andersen et al. (2003), in a parsimonious structure, and has gained popularity in realized variance forecasting. The latter enables forecasting a high-frequency variable using the information of low-frequency variables (Foroni et al., 2018; 2023), providing an appropriate tool for our work. Notably, the HAR model we use is in logarithmic form. This is to avoid generating negative forecasted $\boldsymbol{D}_t$ and to allow for the applicability of standard normal distribution theory (Andersen et al., 2003).

Additionally, the existing body of literature on forecasting asset return volatility using different frequency-based exogenous variables predominantly relies on the GARCH-MIDAS model originally developed by Engle et al. (2013) (see, Amendola et al. (2024) and Segnon et al. (2024) for detailed literature reviews on the various extensions of this framework). However, these studies view volatility as a latent variable instead of the "observable" realized volatility (RV). The latter, based on intraday data, represents a more accurate measurement of volatility (Andersen et al., 2001) and has become a popular proxy for the same in recent years (McAleer and Medeiros, 2008).

As for the realized correlation matrix $\boldsymbol{R}_t$, in order to ensure generation of positive-definite forecasted matrices, we first apply the matrix-logarithm transformation (Chiu et al., 1996) to it. Then, we vectorize its lower off-diagonal elements, and use the scalar MHAR model to conduct forecasting. After that, we utilize the novel approach developed by Archakov and Hansen (2021) to reconstruct the forecasted vectors into logarithmic matrices. The method of Archakov and Hansen (2021) provides a mapping function that can transform any given $N(N-1)/2 \times 1$ vector into the corresponding N-dimensional logarithmic matrix uniquely. Followed by exponentiation, we obtain the forecasted $\widehat{\boldsymbol{R}}_t$. The above approach offers two advantages. Firstly, by leveraging the method proposed by Archakov and Hansen (2021), it ensures the acquisition of positive-definite forecasted realized correlation matrices without any model restrictions. Few studies, such as Arias et al. (2023), Hafner and Wang (2023), and Archakov et al. (2024), also utilize this novel method to model the correlation matrix. Secondly, the scalar MHAR model produces a parsimonious structure (as documented by Bollerslev et al. (2018)), which is of great significance in high-dimensional scenarios.

Our forecasting results demonstrate that, with the exception of the Least absolute shrinkage and selection operator (Lasso)-RM, which accounts for uncertainty of all the 50 states in the model for realized variances ($\boldsymbol{D}_t$), the proposed RM models generally surpass the benchmark models in terms of both forecast losses and portfolio performances. This indicates an enhancement in incorporating the information of the volatility of ECI into the stock covariance forecasting model. Furthermore, we apply the reverse-MIDAS framework to the realized correlation ($\boldsymbol{R}_t$) forecasting model and propose the RM-MHARX model to incorporate the information of the weekly correlation of the ECIs, demonstrating that this enhances the covariance forecasting performance in the DRD framework.

This paper contributes to the literature of RCOV in three aspects: Firstly, we develop a class of RM-HAR models to incorporate the low-frequency variables into the realized volatility forecasting framework. To the best of our knowledge, this is first study to combine the HAR model with the RM framework for forecasting daily realized variances. Our work differs from the only related work, Hecq et al. (2024), who utilize the RM model to introduce the monthly macroeconomic variables to forecast the daily realized variance of the S&P 500, and indicate that most of these variables provide limited forecasting improvement. In contrast, the low-frequency variables employed in our study are at a weekly frequency and achieve significant forecasting enhancement.

Secondly, we introduce the novel correlation matrix parameterization method of Archakov and Hansen (2021) into the realized correlation forecasting exercise for the first time. Our work diverges from prior related studies (e.g., Arias et al., 2023; Hafner and Wang, 2023; Archakov et al., 2024). Although these studies also utilize the novel method of Archakov and Hansen (2021) to model the correlation matrix, they focus on modeling the latent correlation matrix. In contrast, by utilizing the approach of Archakov and Hansen (2021) and the scalar MHAR model, we obtain the positive-definite forecasted correlation matrix without the need for imposing any restrictive model restrictions.

Finally, we investigate the role of ECI-based economic uncertainty in forecasting state-level RCOV of stock returns. The rationale for adopting this regional perspective stems from the premise that core business activities of firms often occur close to their headquarters (Pirinsky and Wang, 2006; Chaney et al., 2012). As a result, equity prices are likely to exhibit a significant regional component, and investors tend to overweight local firms in their portfolios (Coval and Moskowitz, 1999, 2001; Korniotis and Kumar, 2013). Consequently, the forecasting analysis conducted in this study should be of immense value to investors, particularly in informing portfolio allocation decisions.

The remainder of this paper is structured as follows. Section 2 introduces the realized measures, while Section 3 presents the econometric models and its estimation methods. Section 4 reports the data, with Section 5 devoted to the predictive forecast results. Sections 6 and 7 conduct robustness checks and additional analysis wherein dynamic correlation of ECIs are introduced into the scalar MHAR model, respectively. Finally, Section 8 concludes.

2. Realized measures

2.1. Realized covariance matrix

Realized covariance, as proposed by Andersen et al. (2003), is a key concept in financial econometrics, particularly in the risk analysis involving high-frequency trading data. It refers to the empirical estimate of the covariance between the returns of financial assets over a given time period. Unlike traditional covariance measures, which typically rely on daily or lower-frequency data, realized covariance leverages high-frequency data to capture the dynamic co-movement of asset prices with greater precision. For a given data sampling frequency $\triangle$ (e.g., 5 min), $1/\triangle$ observations can be obtained within a trading day. The daily realized covariance matrix $\boldsymbol{S}_t$ is defined as:

$$\boldsymbol{S}_t = \sum_{j=1}^{1/\triangle} \boldsymbol{r}_{t-1+j\cdot\triangle}\, \boldsymbol{r}'_{t-1+j\cdot\triangle}, \quad (1)$$

where $\boldsymbol{r}_t = 100 \times (log\boldsymbol{P}_t - log\boldsymbol{P}_{t-\triangle})$ denotes the log return vector of N assets, and $\boldsymbol{P}_t$ is the price vector. This measure is computed by summing the product of contemporaneous returns across the high-frequency intervals within the time period of interest. The high-frequency nature of the data allows us to capture intraday information, providing a more accurate estimate of the covariance.

2.2. Realized variance, jump and semivariance

Realized variance is actually the element on the diagonal of the aforementioned realized covariance matrix $\boldsymbol{S}_t$. Likewise, it is computed as $RV_t = \sum_{j=1}^{1/\triangle} r_{t-1+j\cdot\triangle}^2$, within r_t denotes the log return. According to Barndorff-Nielsen and Shephard (2004), as the sample frequency $\triangle \rightarrow 0$, the realized variance converges into a continuous component and a discontinuous one. This is expressed as:

$$\lim_{\triangle\rightarrow 0} RV_t = \int_t^{t+1} \sigma^2(s)ds + \sum_{t<s\leq t+1} \kappa^2(s). \quad (2)$$

On the right-hand side of the equation, the first term, the continuous component, is related to the realized bipower variation, which is defined as:

$$BV_t = \mu_1^{-2} \sum_{j=2}^{1/\triangle} |r_{t-1+j\cdot\triangle}||r_{t-1+(j-1)\cdot\triangle}|, \quad (3)$$

where $\mu_1 = \sqrt{2/\pi}$. When $\triangle \rightarrow 0$, there are $BV_t \rightarrow \int_t^{t+1} \sigma^2(s)ds$. The discontinuous component (jump) can therefore be estimated as:

$$\lim_{\triangle\to 0}(RV_t - BV_t) = \sum_{t<s\leq t+1}\kappa^2(s). \tag{4}$$

Barndorff-Nielsen and Shephard (2004) proposed truncating jump measurements to zero to avoid negative values in empirical implementation:

$$J_t = \max(RV_t - BV_t, 0). \tag{5}$$

However, this measure can produce many insignificant jumps, which can lead to noise. Andersen et al. (2007) use the Z-statistic test of Huang and Tauchen (2005) to screen out "large" jumps, denoted as CJ_t in literatures. Specifically, the Z-statistic is computed as:

$$Z_t = \frac{\sqrt{1/\triangle}(RV_t - BV_t)RV_t^{-1}}{\sqrt{(\mu_1^{-4}+2\mu_1^{-2}-5)\cdot\max(1, TQ_t/BV_t^2)}}, \tag{6}$$

where TQ_t is the standardized realized tripower quarticity measure,

$$TQ_t = \triangle^{-1}\,\mu_{4/3}^{-3}\sum_{j=3}^{1/\triangle}\left|r_{t-1+j\cdot\triangle}\right|^{4/3}\left|r_{t-1+(j-1)\cdot\triangle}\right|^{4/3}\left|r_{t-1+(j-2)\cdot\triangle}\right|^{4/3}, \tag{7}$$

where $\mu_{4/3} = 2^{2/3}\Gamma(7/6)\Gamma(1/2)^{-1}$. Then CJ_t is represented by:

$$CJ_t = (RV_t - BV_t)\cdot I(Z_t > \Phi_\alpha), \tag{8}$$

where Φ_α is some critical value under the significance level α, and $I(\cdot)$ denotes the indicator function that takes the value of 1 if $I(\cdot)$ is true and 0 if $I(\cdot)$ is false. Then, the other component of the total realized variance is measured by:

$$CV_t = RV_t - CJ_t = RV_t\cdot I(Z_t < \Phi_\alpha) + BV_t\cdot I(Z_t > \Phi_\alpha), \tag{9}$$

which is continuous.

Additionally, Barndorff-Nielsen et al. (2010) decompose the realized variance into two components, the positive semivariance and the negative semivariance. We also consider using these components in the next section. The positive realized semivariance estimator is written as:

$$PSV_t = \sum_{j=1}^{1/\triangle} r_{t-1+j\cdot\triangle}^2\, I(r_{t-1+j\cdot\triangle} > 0), \tag{10}$$

and the negative semivariance estimator is defined as:

$$NSV_t = \sum_{j=1}^{1/\triangle} r_{t-1+j\cdot\triangle}^2\, I\left(r_{t-1+j\cdot\triangle} < 0\right). \tag{11}$$

3. Forecasting methodology

3.1. The DRD approach for forecasting realized covariance matrix

Inspired by the dynamic condition correlation (DCC) model of Engle (2002), Oh and Patton (2016) proposed a two-step procedure, named DRD approach, to forecast the realized covariance matrix, in which the realized variance and realized correlation matrix are modeled separately. This method has two advantages. Firstly, the computational complexity can be reduced under high dimension conditions since the realized variances can be treated as univariate linear forecasting problem rather than vector modeling problem. Secondly, exogenous predictors can be considered in covariance matrix forecasting by incorporating them into the variance forecasting model. To this end, we adopt the DRD approach to investigate the importance of the economic conditions in covariance matrix forecasting in US state-level stock markets.

According to Oh and Patton (2016), the realized covariance matrix $\boldsymbol{S}_t$ can be decomposed into the DRD form as:

$$\boldsymbol{S}_t = \boldsymbol{D}_t^{1/2} \boldsymbol{R}_t \boldsymbol{D}_t^{1/2}, \tag{12}$$

where $\boldsymbol{D}_t$ is a diagonal matrix with the elements of the realized variances for all assets, i.e., $\boldsymbol{D}_t = diag(\boldsymbol{S}_t) = diag(\{RV_{n,t}\}_{n=1}^{N})$, and $\boldsymbol{R}_t = \boldsymbol{D}_t^{-1/2} \boldsymbol{S}_t \boldsymbol{D}_t^{-1/2}$ denotes the realized correlation matrix. We forecast $\boldsymbol{D}_t$ and $\boldsymbol{R}_t$ separately with different approaches to get their forecasts $\widehat{\boldsymbol{D}}_t$ and $\widehat{\boldsymbol{R}}_t$, and then the realized covariance forecasts $\widehat{\boldsymbol{S}}_t$ can be obtained through $\widehat{\boldsymbol{S}}_t = \widehat{\boldsymbol{D}}_t^{1/2} \widehat{\boldsymbol{R}}_t \widehat{\boldsymbol{D}}_t^{1/2}$.

3.2. Forecasting $\boldsymbol{D}_t$ with reverse- MIDAS framework

Since $\boldsymbol{D}_t$ is a diagonal matrix with the elements of realized variances for the given N assets, we can individually forecast the N-dimensional univariate realized variances to obtain the forecast $\widehat{\boldsymbol{D}}_t$. In particular, we propose several RM-HARX models by combining the reverse-MIDAS (RM) framework of Foroni et al. (2018) and the HAR model of Corsi (2009) with exogenous variables (HARX) together to forecast univariate realized variances. The proposed models allow us to employ the volatility of the weekly state-level ECIs to forecast daily realized variances in US state-level stock markets. In addition, following Andersen et al. (2007), we employ the logarithm HAR-type models to avoid generating negative variance forecasts. The realized variance forecasts can then be recovered via the exponential function. Finally, given the forecasted realized variances $\widehat{RV}_{n,t}$ for n-th state-level stock market index, we can obtain the realized variance matrix forecasts as $\widehat{\boldsymbol{D}}_t = diag(\{\widehat{RV}_{n,t}\}_{n=1}^{N})$. The several proposed univariate variance forecasting models within the RM-HARX class are introduced as follows.

3.2.1. RM-HARX model

The first proposed reverse-MIDAS univariate realized variance forecasting model is constructed by integrating the logarithm HAR model into the reverse-MIDAS framework. Assuming the forecast horizon is h, which is relative to the last timestamp of high-frequency observations, the RM-HARX model is expressed as:

$$\log(RV_{t+\frac{l}{L}+\frac{h}{L}}) = \beta_{0,l} + \beta_{d,l}\log(RV^{d}_{t+\frac{l}{L}}) + \beta_{w,l}\log(RV^{w}_{t+\frac{l}{L}}) + \beta_{m,l}\log(RV^{m}_{t+\frac{l}{L}}) + \alpha_l \log(Vol_t^{ECI}) + \varepsilon_{t+\frac{l}{L}+\frac{h}{L}}, t = 0,1,\dots,T-1, l = 1,2,\dots,L, \quad (13)$$

where T denotes the total number of observations of the low frequency variable Vol_t^{ECI}, and L represents the number of observations of high frequency variable during a low frequency period. The daily, weekly and monthly realized variance (RV_t^d, RV_t^w, and RV_t^m) are computed as, $RV_t^d = RV_t$, $RV_t^w = \frac{1}{5}\sum_{i=0}^{4} RV_{t-i}$, $RV_t^m = \frac{1}{20}\sum_{i=0}^{19} RV_{t-i}$. In the empirical section, Vol_t^{ECI} denotes the volatility of the corresponding state's ECI, which is extracted through the GARCH model (see, Appendix A). Additionally, we specify $L = 5$ since Vol_t^{ECI} is at weekly frequency while the forecasted realized variance is at daily frequency.

3.2.2. RM-HARJX model

Given the nonparametric measurements of the jump component mentioned above, the corresponding time series (J_t) can be directly included as an additional explanatory variable, resulting in the RM-HARJX model, which is described as:

$$\log(RV_{t+\frac{l}{L}+\frac{h}{L}}) = \beta_{0,l} + \beta_{d,l}\log\left(RV^{d}_{t+\frac{l}{L}}\right) + \beta_{w,l}\log\left(RV^{w}_{t+\frac{l}{L}}\right) + \beta_{m,l}\log\left(RV^{m}_{t+\frac{l}{L}}\right) + \gamma_{d,l}\log\left(J_{t+\frac{l}{L}} + 1\right) + \alpha_l \log(Vol^{ECI}_t) + \varepsilon_{t+\frac{l}{L}+\frac{h}{L}}. \quad (14)$$

3.2.3. RM-HARCJX model

Following Andersen et al. (2007), we construct an additional RM-HARCJ model that takes into account the truncated continuous and jump components, as mentioned in Section 2.2. The model is represented as:

$$\log(RV_{t+\frac{l}{L}+\frac{h}{L}}) = \beta_{0,l} + \beta_{d,l}\log\left(CV^{d}_{t+\frac{l}{L}}\right) + \beta_{w,l}\log\left(CV^{w}_{t+\frac{l}{L}}\right) + \beta_{m,l}\log\left(CV^{m}_{t+\frac{l}{L}}\right) + \gamma_{d,l}\log\left(CJ^{d}_{t+\frac{l}{L}} + 1\right) + \gamma_{w,l}\log\left(CJ^{w}_{t+\frac{l}{L}} + 1\right) + \gamma_{m,l}\log\left(CJ^{m}_{t+\frac{l}{L}} + 1\right) + \alpha_l \log(Vol^{ECI}_t) + \varepsilon_{t+\frac{l}{L}+\frac{h}{L}}. \quad (15)$$

3.2.4. RM-HARRSX model

Patton and Sheppard (2015) and Sévi (2014) introduce the positive and negative semivariance developed in Barndorff-Nielsen et al. (2010) into the HAR model. As such, we propose the RM-HARRSX as follows:

$$\log(RV_{t+\frac{l}{L}+\frac{h}{L}}) = \beta_{0,l} + \beta_{d,l}\log\left(PSV^{d}_{t+\frac{l}{L}}\right) + \beta_{w,l}\log\left(PSV^{w}_{t+\frac{l}{L}}\right) + \beta_{m,l}\log\left(PSV^{m}_{t+\frac{l}{L}}\right) + \gamma_{d,l}\log\left(NSV^{d}_{t+\frac{l}{L}}\right) + \gamma_{w,l}\log\left(NSV^{w}_{t+\frac{l}{L}}\right) + \gamma_{m,l}\log\left(NSV^{m}_{t+\frac{l}{L}}\right) + \alpha_l \log(Vol^{ECI}_t) + \varepsilon_{t+\frac{l}{L}+\frac{h}{L}}. \quad (16)$$

The semivariances are also assumed to have heterogeneous structure.

3.2.5. PCA-RM-HARX model

For forecasting realized variance in a certain state's stock market, the above models described above only account for the volatility of the ECI of that state. To explore the predictability of uncertainty emanating from other states, we incorporate the economic condition data from all fifty states into the above realized variance forecasting models. Given the substantial increase in the number of exogenous variables, we employ dimension reduction techniques, specifically Principal Component Analysis (PCA), to mitigate the risk of overfitting. The following is the proposed PCA-RM-HARX model:

$$\log(RV_{t+\frac{l}{L}+\frac{h}{L}}) = \beta_{0,l} + \beta_{d,l}\log(RV^{d}_{t+\frac{l}{L}}) + \beta_{w,l}\log(RV^{w}_{t+\frac{l}{L}}) + \beta_{m,l}\log(RV^{m}_{t+\frac{l}{L}}) +$$

$$\alpha_l Factor_t + \varepsilon_{t+\frac{l}{L}+\frac{h}{L}}, t = 0,1,\ldots,T-1, l = 1,2,\ldots,L, \tag{17}$$

where $Factor_t$ is the first principal component extracted from the log volatilities of ECIs for all fifty states, i.e., $(\log(Vol_{n,t}^{ECI}))_{n=1,2,\ldots,50}$. Similarly, we can obtain the PCA versions of the RM-HARJX, RM-HARCJX, and RM-HARRSX models. For the sake of brevity, we omit the corresponding descriptions here.

3.2.4. Lasso-RM-HARX models

We also employ the Lasso approach introduced by Tibshirani (1996) to perform variable selection and alleviate the over-fitting problem. Particularly, we apply the Lasso approach to shrink the low frequency variables, rather than all independent variables.

Let $y_t = \log(RV_t)$, $\boldsymbol{Z}_t = (1, \log(RV_t^d), \log(RV_t^w), \log(RV_t^m))'$, and $\boldsymbol{X}_t$ contains $(\log(Vol_{n,t}^{ECI}))_{n=1,2,\ldots,50}$ indicating the log volatility of ECI of all fifty states. Then the RM-HARX model can be re-written as:

$$y_{t+\frac{l}{L}+\frac{h}{L}} = \boldsymbol{\beta}_l' \boldsymbol{Z}_{t+\frac{l}{L}} + \boldsymbol{\alpha}_l \boldsymbol{X}_t + \varepsilon_{t+\frac{l}{L}+\frac{h}{L}}, \tag{18}$$

where $\boldsymbol{\beta}_l = (\beta_{0,l}, \beta_{d,l}, \beta_{w,l}, \beta_{m,l})'$. Noteworthy, the coefficients of exogenous variables are denoted as $\boldsymbol{\alpha}_l$, distinct from the previously mentioned α_l, since $\boldsymbol{X}_t$ now includes fifty exogenous variables, rather than just one. The parameter estimates of the model obtained through the Lasso method are given by:

$$(\boldsymbol{\beta}_l, \boldsymbol{\alpha}_l) = argmin \sum_{t=0}^{T-1} \left(y_{t+\frac{l}{L}+\frac{h}{L}} - \boldsymbol{\beta}_l{}' \boldsymbol{Z}_{t+\frac{l}{L}} - \boldsymbol{\alpha}_l \boldsymbol{X}_t \right)^2 + \lambda_l(|\boldsymbol{\alpha}_l|), \tag{19}$$

where the tune parameter λ_l is chosen by tenfold cross-validation via the glmnet R package (Friedman et al., 2010) in our empirical part. We refer to this model as Lasso-RM-HARX. The specifications of the Lasso-RM-HARJX model, the Lasso-RM-HARCJX model, and the Lasso-RM-HARRSX model are similar to that of the Lasso-RM-HARX model, the only difference is that $\boldsymbol{Z}_t$ includes different realized measures (e.g., jumps and realized semivariances). We also omit them here.

3.3. Forecasting $\boldsymbol{R}_t$ with the scalar MHAR model and a new parameterization of Archakov and Hansen (2021)

We employ the scalar MHAR to model the realized correlation matrix, which has been adopted in previous literature such as Bollerslev et al. (2018) and Li et al. (2024). The HAR model of Corsi (2009) has become the most widely used framework in the univariate realized volatility forecasting. It was first extended to a multivariate setting by Chiriac and Voev (2010) and later formalized as scalar multivariate HAR (MHAR) model in Bollerslev et al. (2018). However, using the scalar MHAR model to forecast correlation matrix without imposing restrictions may result in non-positive definite matrices.

For the purpose to guarantee the positive definiteness of the forecasted realized correlation matrices $\widehat{\boldsymbol{R}}_t$, we can utilize the matrix logarithm of Chiu et al. (1996) to model the lower triangular part of $\log(\boldsymbol{R}_t)$, including the diagonal, and then reconstruct it by matrix exponentiation. However, this method does not guarantee that the diagonal elements of the reconstructed correlation matrix will be equal to one. For an N-dimensional correlation matrix $\boldsymbol{R}_t$, there are $N \times (N-1)/2$ unique elements whereas $\log(\boldsymbol{R}_t)$ contains $(N+1) \times N/2$ original parameters. When $N = 2$, finding a determinate mapping function between $\mathbb{R}^{(N+1) \times N/2}$ and $\mathbb{R}^{N \times (N-1)/2}$ is relatively straightforward, but it becomes significantly more challenging when $N > 2$. For example, applying the matrix-logarithm to an 2×2 correlation matrix gives, $\log\begin{pmatrix} 1 & \rho \\ \rho & 1 \end{pmatrix} = \begin{pmatrix} \frac{1}{2}\log(1-\rho^2) & \frac{1}{2}log\frac{1+\rho}{1-\rho} \\ \frac{1}{2}log\frac{1+\rho}{1-\rho} & \frac{1}{2}\log(1-\rho^2) \end{pmatrix}$. Archakov and Hansen (2021) developed a novel method for correlation matrix parameterization, which effectively resolves this issue. Their approach enables the reconstruction of the N-dimensional correlation matrix from any given vector in $\mathbb{R}^{N \times (N-1)/2}$ using a mapping function. For further details, refer to Archakov and Hansen (2021).

We combine the novel reconstruction method of Archakov and Hansen (2021) and the scalar MHAR model to get the forecasted positive definite correlation matrices as the following steps. Firstly, by employing the $vech$ operator, we stack the lower off-diagonal elements of an N-dimensional log correlation matrix $\boldsymbol{A}_t = \log(\boldsymbol{R}_t)$ into an $N(N-1)/2 \times 1$ vector $vech(\boldsymbol{A}_t)$. Secondly, modeling and forecasting $vech(\boldsymbol{A}_t)$ with the scalar MHAR model as:

$$vech(\boldsymbol{A}_{t+h}) = \boldsymbol{c} + \theta_d vech(\boldsymbol{A}_t^d) + \theta_w vech(\boldsymbol{A}_t^w) + \theta_m vech(\boldsymbol{A}_t^m) + \boldsymbol{\epsilon}_{t+h}, \quad (20)$$

where $\boldsymbol{c}$ is an $N(N-1)/2 \times 1$ vector denoting the intercept term, θ_d, θ_w and θ_m are scalar parameters. Moreover, $\boldsymbol{A}_t^d = \log(\boldsymbol{R}_t^d)$, and $\boldsymbol{A}_t^w$, $\boldsymbol{A}_t^m$ are similarly, and $\boldsymbol{R}_t^d$, $\boldsymbol{R}_t^w$, $\boldsymbol{R}_t^m$ are decomposed from the daily, weekly, and monthly realized covariance matrices based on the DRD decomposition, e.g., $\boldsymbol{R}_t^d = {\boldsymbol{D}_t^d}^{-1/2} \boldsymbol{S}_t^d {\boldsymbol{D}_t^d}^{-1/2}$. Noteworthy, t represents high-frequency time here (i.e., daily in this paper) rather than low-frequency time as in the aforementioned reverse-MIDAS models. Finally, the forecasts of the correlation matrix, $\widehat{\boldsymbol{R}}_t$, can be uniquely reconstructed from the forecasts of $vech(\boldsymbol{A}_{t+h})$ using the mapping function of Archakov and Hansen (2021). The above correlation matrix forecasting framework ensures the generation of positive definite matrices forecasts, in the meantime, without imposing any restrictions. To the best of our knowledge, this study is the first to integrate the novel parameterization method of Archakov and Hansen (2021) into the realized correlation matrix modeling and forecasting.

[Insert Figure 1 here]

For clarity, we plot the above RCOV forecasting procedure in Figure 1. As illustrated, after getting the forecasts of $\boldsymbol{D}_t$ and $\boldsymbol{R}_t$, the covariance forecasts $\widehat{\boldsymbol{S}}_t$ can be obtained through the combination of $\widehat{\boldsymbol{D}}_t$ and $\widehat{\boldsymbol{R}}_t$ such that $\widehat{\boldsymbol{S}}_t = \widehat{\boldsymbol{D}}_t^{1/2} \widehat{\boldsymbol{R}}_t \widehat{\boldsymbol{D}}_t^{1/2}$. It is important to note that when the forecast horizon is greater than one, we use the direct forecast approach instead of the iterated one, as in Bollerslev et al. (2018) and Wilms et al. (2022). The advantage of this approach is that the direct approach is more robust when dealing with model mis-specifications (Marcellino et al., 2006). Specifically, for the forecast horizon h, the dependent variable in the univariate HAR model (realized variance) and the dependent variable in the scalar MHAR model (realized correlation matrix) are both derived using the DRD approach from the average of the covariance matrix over the future h days. For clarity, we denote the covariance forecasting model as RM-HARX-DRD, which is constructed through the two-step forecasting process based on the variance forecast model RM-HARX and the correlation matrix forecasting model scalar MHAR. Other extended models are denoted similarly. Table 1 presents a summary of the composition of all realized covariance matrix forecasting models. The descriptions of all the forecasting models mentioned above are presented in Table B1 in Appendix B.

[Insert Table 1 here]

4. Data

We source the US state-level stock market indices data at a 5-minute frequency from the Bloomberg database. These indices are constructed by Bloomberg as capitalization-weighted aggregates of equities domiciled in each respective state. Then, we use the aforementioned realized measures to construct various daily-frequency variables. The weekly ECIs of the US states, on which we apply the GARCH model, are based on the work of Baumeister et al. (2024).[2] These authors derive the indices from mixed-frequency Dynamic Factor Models (DFMs) with weekly, monthly, and quarterly variables that cover multiple dimensions of the aggregate and the state economies. Specifically, Baumeister et al. (2024) group variables into six broad categories: mobility measures, labor market indicators, real economic activity, expectations measures, financial indicators, and household indicators. The indexes are scaled to 4-quarter growth rates of US real Gross Domestic Product (GDP) and normalized such that a value of zero indicates national long-run growth. The range of our data covers the period from April 04, 2016, to June 30, 2024. Since our reverse-MIDAS models require a fixed frequency mismatch $L = 5$, we follow the approach of Hecq et al. (2024) and interpolate additional values for any missing daily observations on workdays (Monday to Friday), resulting in 2150 and 430 observations for each daily and weekly variables, respectively. Moreover, we follow the approach of Callot et al. (2017) and Alves et al. (2024) to deal with the extreme values in the daily realized covariance matrices. Specifically, we flag for censoring any covariance matrix where

[2] Table 1 in their paper summarize the state-level data that they use in the construction of the weekly ECIs, and also include information on the frequency, source, transformation, seasonal adjustment, and the start date of each underlying data series utilized in the construction of the indexes. The data is publicly available for download from: https://sites.google.com/view/weeklystateindexes/dashboard.

more than 25% of the unique entries deviate by more than four standard errors (based on the series corresponding to that entry) from their sample average up to that point. These flagged matrices are then replaced with the average of the nearest five preceding and following non-flagged matrices.

[Insert Figure 2 here]

In the empirical section, we primarily concentrate on a ten-dimensional covariance matrix forecasting scenario. The ten state-level stock indices used to construct the RCOV are randomly selected similar to Bollerslev et al. (2018), Opschoor et al. (2018), and Opschoor et al. (2024). In this regard, Table C1 in Appendix C lists the names of the chosen states. In a robustness check, we examine the out-of-sample forecast precision within higher-dimensional contexts of 20, 30, 40 and all of the 50 states. In Figure 2, we plot the autocorrelation function (ACF) for the logarithm realized variances of ten chosen state-level stock market indices. It is evident that the ACF decays gradually across all assets after the first few lags, indicating significant autocorrelation and long memory. This phenomenon is very common in volatility time series and suggests that past variances are informative for predicting future variances. Given that the HAR model is a straightforward and effective tool for capturing long memory in volatility forecasting, we integrate the reverse-MIDAS framework into the HAR model to forecast the realized variances.

[Insert Figure 3 here]

We also depict the time series of the logarithm realized variances and the logarithm volatilities of ECIs of the corresponding states in Figure 3. It can be easily seen that the two series have very similar characteristics. For instance, both indicate peaks around April 2020 and April 2021, while displaying less fluctuation during the remaining periods. According to Figure 3, there appears to be a notable connection between the two series. This suggests that we may be able to leverage this relationship for forecasting purposes. In the next section, we will investigate this further by examining in-sample fitting and out-of-sample forecasting in greater detail.

5. Empirical findings

We evaluate the forecast models by comparing various HAR-DRD models and their reverse-MIDAS version (which takes into account the information of volatility involving economic conditions) relying on statistical and economic criteria. We first present the in-sample parameter estimate results and assess the in-sample fits in sub-section 5.1., and then analyze the out-of-sample forecast performance in sub-section 5.2.

5.1. In-sample fits

We begin by presenting the full-sample parameter estimates for each pair of the reverse-MIDAS (RM) and non-RM HAR-type univariate variance forecasting models in Tables 2-4, corresponding to $h = 1$, 5, and 20, along with standard errors in parentheses. To save space, we follow the approach of Bollerslev et al. (2018) and report the averages of the model parameter estimates and standard errors for the ten selected states. Additionally, since the reverse-MIDAS models need to be re-estimated every workday, their estimates are further averaged over five workdays. From Table 1-3, it can be observed that the daily, weekly, and monthly lag terms are significantly positive in all models. Besides, for each class of HAR(X) models, the reverse-MIDAS frameworks always have higher adjusted R^2, which represents better in-sample-fit performance. It is noteworthy that the standard errors of estimates for the exogenous variable involving volatility of the ECI are relatively large, in comparison to their coefficients α, when $h = 1$. However, these standard errors become relatively smaller when $h = 5$ and 22. In other words, the estimated coefficients α exhibit less statistical significance in short-term, while they become relatively more statistically significant in the medium- to long-term. Meanwhile, for all forecast horizons, the estimated coefficients α are positive, indicating that an increase in the volatility of the ECI leads to higher future volatility in state stock markets. This aligns with expectations, as heightened economic uncertainty typically drives market volatility. Additionally, with the inclusion of ECI volatility, the coefficient of the monthly realized variance component, β_m, gets significantly reduced, suggesting that ECI volatility can partially replace the influence of long-term volatility of stock markets.

[Insert Tables 2, 3 and 4 here]

5.2. Statistical evaluation of out-of-sample forecasts

Next, we use four types of statistical loss functions to evaluate the out-of-sample forecasting accuracy of the realized covariance forecasting models, including Euclidean, Frobenius, and QLIKE according to Symitsi et al. (2018) as well as the Stein loss function according to Laurent et al. (2012) and Luo and Chen (2020). Given the realized covariance matrix forecast $\widehat{\boldsymbol{S}}_t$, the Euclidean loss function is expressed as:

$$L_t^{Eucl} = \sqrt{vech(\boldsymbol{S}_t - \widehat{\boldsymbol{S}}_t)'vech(\boldsymbol{S}_t - \widehat{\boldsymbol{S}}_t)}, \quad (21)$$

and the Frobenius loss function is expressed as,

$$L_t^{Frob} = \sqrt{Tr[(\widehat{\boldsymbol{S}}_t - \boldsymbol{S}_t)(\widehat{\boldsymbol{S}}_t - \boldsymbol{S}_t)']}, \quad (22)$$

where $Tr(\cdot)$ represents the trace of a matrix. The QLIKE function is given as:

$$L_t^{QLIKE} = \log|\widehat{\boldsymbol{S}}_t| + Tr(\widehat{\boldsymbol{S}}_t^{-1}\boldsymbol{S}_t), \quad (23)$$

the Stein loss function is as follows:

$$L_t^{Stein} = Tr(\widehat{\boldsymbol{S}}_t^{-1}\boldsymbol{S}_t) - \log|\widehat{\boldsymbol{S}}_t^{-1}\boldsymbol{S}_t| - K. \quad (24)$$

Following Bollerslev et al. (2018), we also adopt the MCS test (Hansen et al., 2011) and the DM test (Diebold and Mariano, 1995) to evaluate whether differences in forecast accuracy for the competing models are statistically significant. The MCS test is used to identify superior models from the set of candidate models, while the DM test is applied to compare the performance of various HAR-DRD models and their reverse-MIDAS versions, which incorporate the volatility of the ECI.

Our out-of-sample forecast comparisons are based on three forecast horizons, i.e., short ($h = 1$), medium ($h = 5$), and long ($h = 20$). We continue to use the same ten-dimensional covariance matrix analyzed earlier and forecast the $\boldsymbol{D}_t$ and $\boldsymbol{R}_t$ separately using the method described above. These forecasts are then combined to reconstruct the covariance matrix forecasts. All models are re-estimated daily based on a rolling window sample of approximately five years (i.e., 260 weeks). It is important to note that our goal is not to run a horse-race between the different models to find a single best model. Instead, we aim to explore whether integrating the low-frequency predictors into the RM, PCA-RM and Lasso-RM models enhances their performance compared to their non-RM benchmark counterparts. Table 5 reports the out-of-sample performance metrics for all covariance matrix forecasting models. For clarity, we categorize the models into four groups based on the four types of HAR models, i.e., HAR, HARJ, HARCJ and HARRS models.

We apply the Model Confidence Set (MCS) of Hansen et al. (2011) to determine whether the forecast accuracy differs significantly across the competing models. For each of the four loss functions and three forecast horizons, we determine the subset of models that are included in the MCS at 75% confidence level, which are highlighted in bold. Additionally, to investigate whether incorporating the volatility of economic conditions improves the performance of the forecasting models, we conduct pairwise comparisons between each RM-based model and its corresponding non-RM benchmark model using the Diebold-Mariano (DM) test (Diebold and Mariano, 1995). Statistical significance is indicated by an asterisk.

[Insert Table 5 here]

According to Table 5, for the short horizon, both PCA-RM-HARX-DRD, RM-HARJX-DRD, and PCA-RM-HARJX-DRD, are included in the MCS across all loss functions. Additionally, the RM-HARX-DRD and PCA-RM-HARCJX-DRD are also included in the MCS for QLIKE- and Stein-type losses. However, nearly all Lasso-RM models are excluded from the MCS, suggesting poor out-of-sample performances. Across all model groups, those in Group 2, which incorporates the jump component, are more likely to be included in the MCS compared to models in other groups. The DM test results show that most RM models, except for the Lasso-RM models, outperform their respective benchmark models within each group. This is especially evident for the PCA-RM models.

For the medium-term horizon (h=5), the advantage of PCA-RM models persists, as nearly all PCA-RM models—except for PCA-RM-HARCJX-DRD—are included in the MCS across all loss functions. Again, the Lasso-RM models fail to make it into the

MCS, reinforcing the notion that their structure does not efficiently capture medium-term volatility dynamics. The DM test results provide further evidence that the RM and PCA-RM models consistently outperform their non-RM counterparts. The results suggest that incorporating economic uncertainty at the weekly level enhances covariance forecasting accuracy over medium horizons, likely because economic conditions unfold over a longer timeframe and contribute to persistent market trends.

Regarding the long forecast horizon, the findings are similar to those for shorter horizons. The RM models and the PCA-RM models generally exhibit better forecasting performance than their benchmark non-RM models, as indicated by the DM test results. However, the Lasso-RM models continue to perform poorly. Notably, the performance of PCA-RM models appears slightly worse than that of the RM models which only consider the volatility of the corresponding state when compared to their benchmarks. For instance, PCA-RM models consistently outperform their benchmarks only in Group 3 across all loss functions, whereas RM models outperform their benchmarks in all groups. Conversely, PCA-RM models, which incorporate the ECI volatilities of all fifty states, show a slight advantage over RM models for $h = 1$. This suggests that considering the volatilities of other ECIs provides clear benefits for short-term covariance matrix forecasting, but these benefits diminish as the forecasting horizon lengthens.

Across all forecast horizons, models in Group 2, which incorporate jump components, consistently demonstrate superior predictive performance, as evidenced by their frequent inclusion in the MCS. This highlights the importance of capturing discontinuities in realized variance when forecasting covariance matrices, as market shocks and sudden changes in volatility significantly influence future covariance structures. The overall findings suggest that incorporating economic uncertainty—particularly through RM and PCA-RM models—enhances forecasting accuracy, especially in the short- and medium-term horizons. However, the benefits of integrating uncertainty measures from multiple states appear to diminish over longer horizons, emphasizing the importance of selecting appropriate predictors for different forecast periods.

[Insert Figure 4 here]

Figure 4 depicts the average rankings of each model across the three forecast horizons for the four loss functions, represented by lines of different colors. Lower rankings indicate better performance, meaning that models closer to the center of the graph perform more effectively. For each group of models, it is evident that the RM model and PCA-RM model are positioned closer to the center of the graph compared to the Lasso-RM model and the benchmark models. Moreover, the PCA-RM model emerges as the top performing model in most cases. Additionally, models in Groups 1 and 2 are generally closer to the center than those in other groups. Among all competing models, the Lasso-RM models consistently rank the farthest from the center of the graph.

In sum, the out-of-sample results show that the RM and RM-PCA models significantly outperform their non-RM counterparts, especially for the medium and long horizons. This indicates that using the information embedded in the lower frequency variable involving volatility of economic conditions capturing uncertainty does help to improve state-level stock market covariance forecasting. Notably, both PCA-RM and Lasso-RM models account for economic volatility across all 50 states, yet their performance differs substantially. While the PCA-RM model outperforms benchmark models, the Lasso-RM model fails to reach a comparable level of accuracy. A potential technical explanation for this discrepancy is the difficulty the Lasso estimator faces in convergence and in selecting the optimal tuning parameter during empirical implementation. Intuitively, this finding underscores the importance of common factor movements over idiosyncratic variations in ECI volatility across states. Among all competing models, the RM-HARJX-DRD model stand out as always being included in the MCS, regardless of the loss functions and forecasting horizons, indicating prevailing forecasting accuracy, highlighting the importance of the jump component in accurately modeling the volatility dynamics (Caporin et al., 2016).

5.3. Economic evaluation

The out-of-sample results presented above show that the RM and PCA-RM models, which incorporate the volatility of economic conditions of the US states, outperform their benchmark models in terms of forecast accuracy. In this sub-section, we focus on investigating whether the proposed models can produce higher economic gains. Following the approach in Bollerslev et al. (2018), Luo and Chen (2020) and Li et al. (2024), we assess the economic performance of the various covariance forecasting models by constructing Global Minimum Variance (GMV) portfolios. As highlighted by Bollerslev et al. (2018), the GMV weights depend solely on return covariances, offering a particularly clear framework for assessing the effectiveness of different models. This approach avoids reliance on forecasts of expected returns, ensuring that the evaluation focuses exclusively on the performance of covariance forecasts. Moreover, as noted by Jagannathan and Ma (2003) and DeMiguel et al. (2009), mean-variance optimized portfolios typically underperform GMV portfolios in terms of out-of-sample Sharpe ratios, primarily due to the estimation error in expected returns, which can distort portfolio positions. Thus, we rely on the GMV portfolio approach to evaluate the economic performance of the competing forecasting models.

Specifically, given the return covariance matrix forecasts $\widehat{\boldsymbol{S}}_t$ for the N chosen assets, a risk-averse investor minimizes the conditional volatility by solving the following global minimum variance portfolio problem:

$$\boldsymbol{w}_t = \arg\min \boldsymbol{w}_t' \widehat{\boldsymbol{S}}_t \boldsymbol{w}_t, \quad (25)$$
$$s.t. \boldsymbol{w}_t' l = 1,$$

where l is a $N \times 1$ vector of ones. The optimal solution of the above problem is written as:

$$\boldsymbol{w}_t = \frac{\widehat{\boldsymbol{S}}_t^{-1} l}{l' \widehat{\boldsymbol{S}}_t^{-1} l} \quad (26)$$

In the following, we denote the *n*-th element of $\boldsymbol{w}_t$ corresponding to the allocation to the *n*-th asset as $w_{n,t}$. We also denote the return on the *n*-th asset by $r_{n,t}$. Then, we can obtain the portfolio return by:

$$r_{pt} = \boldsymbol{w}_t' \boldsymbol{r}_t. \quad (27)$$

We report the annualized return in this paper which is calculated as:

$$Annu\ Return = 100 \times [(1 + r_{pt})^{252} - 1]. \tag{28}$$

The Sharpe ratio is widely employed in the academic research for assessing portfolio performance by balancing risk and return. Based on the portfolio returns established above, the standard deviation of the portfolio σ_p is computed using:

$$\sigma_p = \sqrt{\frac{1}{T_2}\sum_{t=T_1+1}^{T}\left(r_{pt} - \frac{1}{T_2}\sum_{t=T_1+1}^{T} r_{pt}\right)^2}, \tag{29}$$

where T_2 is the length of out-of-samples. The Sharpe ratio indicates the ratio of average returns over risks as follows:

$$Sharp = \frac{r_p}{\sigma_p} = \frac{\frac{1}{T_2}\sum_{t=T_1+1}^{T} r_{pt}}{\sigma_p}. \tag{30}$$

In practice, evaluating a portfolio's diversification requires assessing whether it is heavily weighted in a few assets. If certain individual assets are overweighted, the portfolio becomes more susceptible to abnormal fluctuations, increasing overall risk. To address this, we also report the portfolio concentration levels, which are expressed as:

$$CO_t = \left(\sum_{n=1}^{N} w_{n,t}^2\right)^{1/2}. \tag{31}$$

Since short selling incurs extra costs, we also report the portfolio short position by:

$$SP_t = \sum_{n=1}^{N} w_{n,t} \cdot I(w_{n,t} < 0). \tag{32}$$

A larger short position indicates a higher proportion of short selling within the portfolio, which, in turn, increases leverage and potentially amplifies risk. Additionally, fewer and less extreme short positions enhance the feasibility of implementing the portfolio in practice.

Moreover, following Callot et al. (2017), Bollerslev et al. (2018), and Luo et al. (2022), we consider the utility-based framework of Fleming et al. (2001, 2003) to evaluate the economic value of the different forecasting models. Specifically, if the investor has quadratic utility with risk aversion γ, the realized utility generated by the portfolio based on the covariance forecasts from model k, can be expressed as:

$$U(r_{pt}^k, \gamma) = (1 + r_{pt}^k) - \frac{\gamma}{2(1+\gamma)}(1 + r_{pt}^k)^2, \tag{33}$$

and the economic value of the model k and model l therefore be determined by solving for $\Delta\gamma$ in the following equation:

$$\sum_{t=T_1+1}^{T} U\left(r_{pt}^{k}, \gamma\right) = \sum_{t=T_1+1}^{T} U\left(r_{pt}^{l} - \Delta\gamma, \gamma\right). \quad (34)$$

The greater the $\Delta\gamma$, the more returns that a risk-aversion investor would like to sacrifice to switch from model l to model k.

[Insert Tables 6, 7 and 8 here]

Tables 6-8 report the portfolio performance, in terms of the above indicators, for different covariance forecasting models and various horizons. Firstly, for the short horizon, as reported in Table 6, the RM model in each group exhibit superiority relative to their benchmark model in terms of annualized returns, economic value and Sharpe ratio. The RM-HARCJX-DRD model achieves the highest annualized return of 8.137% and the highest Sharpe ratio, as indicated in bold in Table 6. Generally, regardless of whether γ is equal to 1 or 10, risk-averse investors tend to accept lower returns in favor of transitioning from benchmark models to the RM-class models. Moreover, the PCA-RM models also demonstrate relatively lower portfolio short positions (in absolute value) compared to the benchmarks, enhancing their practical applicability. Consistent with the statistical evaluations, the Lasso-RM models underperform across nearly all metrics.

As shown in Table 7, for the medium horizon, all RM models still outperform their benchmark models in terms of portfolio annualized returns, economic value, and the Sharpe ratio. Moreover, they demonstrate improved performance in managing short positions. Besides, the Lasso-RM models also have relatively higher returns in the medium-term forecasts. In terms of portfolio concentration and short positions, the PCA-RM models outperform the benchmark models, suggesting that portfolios based on these models are less prone to extreme concentration in specific assets, thereby reducing overall risk exposure. Moreover, implementing short positions typically incurs higher costs compared to long positions, making models that limit excessive shorting more practical and cost-effective.

As shown in Table 8, there are similar findings for the long-run forecasting case compared to the short- and medium-term. For example, all RM class models achieve higher annualized returns, Sharpe ratios, and positive economic values. Moreover, they outperform their benchmark models in managing portfolio short positions. The PCA-RM models continue to show an advantage over their benchmarks, not only in reducing short positions but also in lowering portfolio standard deviation, further enhancing risk management.

In conclusion, portfolios constructed using RM covariance matrix forecasting models consistently achieve higher returns and Sharpe ratios. Figure 5 illustrates the average model rankings across different forecast horizons based on various economic evaluation criteria. Lower rankings indicate superior performance, meaning the closer a model is to the center of the graph, the better its overall effectiveness. As can be seen, the RM models are superior to the benchmark models in terms of annualized returns and Sharpe ratio, and the portfolios constructed based on the PCA-RM models generally perform best in terms of concentrations and short positions. Conversely, the Lasso-RM models exhibit poor performance as they are located farthest from the center of the graph in most cases.

[Insert Figures 6, 7, and 8 here]

In addition, we depict the accumulated returns, which is calculated as: $100 \times \prod_{t=T_1+1}^{T}(1 + r_{pt})$, in Figures 6-8. For clarity, we plot them separately based on the groups. This is because when all sixteen models are presented in a single figure, it becomes extremely difficult to discern the individual lines corresponding to each model. Simultaneously, our principal objective is to conduct a comparative analysis between the reverse-MIDAS models and the benchmark models, rather than identifying the superior model among all competing models.

As shown in the figures, the RM-HAR model (the blue line) in each group demonstrates higher cumulative returns than the benchmark model (the red lines) irrespective of the forecast horizons. Moreover, in the medium-term, the portfolios constructed using the Lasso-RM models yield the highest accumulated returns within each group. However, over the long-term, portfolios based on the Lasso-RM forecasting models have clearly lower accumulated returns compared to other competing models.

Meanwhile, portfolios built on PCA-RM models generally produce cumulative returns similar to those of the benchmark models, with only slight deviations either above or below them. The results shown in Figures 5 to 7 further strengthens the economic advantages of using the reverse-MIDAS covariance matrix forecasting models which incorporates exogenous low-frequency volatility of economic conditions as concluded in Tables 6-8.

6. Robustness checks

6.1. *Alternative RCOV measure: MRK*

Our analysis demonstrates that the RM and PCA-RM models, which take into account the information of the volatility of economic conditions, outperform their benchmark counterparts in forecasting the covariance matrix. To assess the robustness of these findings, we employ an alternative covariance measure—the multivariate realized kernel (MRK; Barndorff-Nielsen et al., 2011)—to calculate the realized covariance matrix for the 10 state-level stock market indices.

As outlined by Barndorff-Nielsen et al. (2011), the multivariate realized kernel (MRK), which takes trading noise and non-synchronicity into account, is expressed as follows:

$$\boldsymbol{S}_t^{MRK} = \sum_{h=-n}^{n} k\left(\frac{h}{H}\right)\gamma_h, \tag{35}$$

where γ_h is the h-th realized autocovariance, i.e., $\sum_{j=h+1}^{n}\boldsymbol{r}_j\boldsymbol{r}'_{j-h}$ for $h \geq 0$, and $\gamma_h = \gamma'_{-h}$ for $h < 0$. As recommended in Barndorff-Nielsen et al. (2011), we employ the Parzen kernel function to represent the function $k(\cdot)$ as due to its simplicity.

Table C2 of Appendix C shows the out-of-sample forecasting result of the alternative covariance measure, MRK, using the abovementioned covariance forecasting models. The results clearly indicate that the RM and PCA-RM models outperform their benchmark models in all groups, demonstrating strong overall performance. Specifically, the PCA-RM-HARX-DRD and the PCA-RM-HARJX-DRD models are always included in the MCS across different loss functions and forecast horizons. However, the four Lasso-based models continue to generally perform poorly.

These findings confirm that our primary results remain robust, regardless of the covariance measure used.

6.2. *Alternative dimension of covariance matrices: N=20 and 30*

In this sub-section, we assess the robustness of the previous conclusions by considering higher-dimensional covariance matrices. We construct covariance matrices using stock market indices for 20, 30, 40 (with the selected states shown in Table C1 of Appendix C) and all the 50 states and employ the forecasting method outlined in the previous section to obtain RCOV forecasts. The forecasting losses for the 20-, 30-, 40-, and 50-dimensional covariance matrix are presented in Tables C3, C4, C5, and C6 of Appendix C, respectively. As we can see from these tables, similar findings are obtained to those previously derived under the case of 10 states. The RM and PCA-RM models generally produce better performances than the benchmark models. Moreover, the PCA-RM-HARX-DRD and the PCA-RM-HARJX-DRD are almost always included in the MCS, regardless of loss functions and forecast horizons.

6.3. *Alternative volatility model for ECIs: Using SV model to extract the volatility of ECIs*

In this sub-section, we replace the volatility extracted from ECIs via the GARCH model with the stochastic volatility (SV) model (see, Appendix A), By still using the original approach of calculating the covariance matrix, and forecasting methods outlined in the previous section, the corresponding out-of-sample forecasting results are presented in Table C7 of Appendix C. The findings remain consistent—both the RM and PCA-RM models in each group outperform their benchmark counterparts, whereas the Lasso-RM models continue to underperform.

6.4. *Alternative out-of-sample period*

The choice of the out-of-sample range can influence the conclusions of the experiments. To ensure the robustness of our results, we extend our analysis to an alternative and earlier out-of-sample period, spanning from October 18, 2016, to March 29, 2021, while maintaining the full-sample start date of October 24, 2011. In contrast, the original out-of-sample range covered March 30, 2021, to June 30, 2024. We then reapply the forecasting procedure using this revised timeframe. The corresponding forecasting losses are reported in Table C8 of Appendix C. Once again, our findings remain unchanged—both the RM and PCA-RM models consistently outperform the non-RM benchmark models in forecast accuracy, while the Lasso-RM models continue to exhibit weak performance.

7. *Further analysis: introducing dynamic correlations of ECIs into the scalar MHAR model*

In the previous sections, we forecasted the realized correlation matrix $\boldsymbol{R}_t$ with the scalar MHAR model. Although our investigation of the role of the ECI in RCOV forecasting mainly relies on incorporating the volatility of the ECI into the realized variance forecasting models. As a supplementary, we also integrate the information from the ECIs into the realized correlation matrix forecasting model. Particularly, we forecast the realized correlation matrix of the state-level stock market by utilizing the correlation of the state-level ECIs, which is estimated by the DCC-GARCH model (see, Appendix A) of Engel (2002). Since the time-varying correlation matrix of ECIs is at weekly frequency while the realized correlation matrix of stock market is daily, we combine the scalar MHAR with the reverse-MIDAS model like the models for realized variance introduced in Section 3.

Consider the scalar MHAR model in section 3, we now specify it in a reverse-MIDAS framework as follows:

$$vech(\boldsymbol{A}_{t+\frac{l}{L}+\frac{h}{L}}) = \boldsymbol{c}_l + \theta_{d,l} vech(\boldsymbol{A}^d_{t+\frac{l}{L}}) + \theta_{w,l} vech(\boldsymbol{A}^w_{t+\frac{l}{L}}) + \theta_{m,l} vech(\boldsymbol{A}^m_{t+\frac{l}{L}+\frac{h}{L}}) + \alpha_l vech(\boldsymbol{CX}_t) + \boldsymbol{\epsilon}_{t+\frac{l}{L}+\frac{h}{L}}, t = 0,1,\dots,T-1, l = 1,2,\dots,L, \quad (36)$$

where $\boldsymbol{A}_t = \log(\boldsymbol{R}_t)$, $\boldsymbol{CX}_t = \log(\boldsymbol{Corr}_t^{ECI})$, and $\boldsymbol{Corr}_t^{ECI}$ represent the dynamic correlation matrix of state-level ECIs estimated via the DCC-GARCH model. The model integrates the dynamic correlations of ECIs into the stock market realized correlation matrix forecasting, and we denote it as scalar RM-MHARX model for convenience.

[Insert Table 9 here]

Table 9 shows the in-sample estimate of the scalar MHAR model and its RM version for three forecast horizons based on the whole sample. As observed, the coefficients for the daily, weekly and monthly lags are significantly positive. Moreover, the adjusted R^2 of RM-MHARX model is slightly higher than that of its benchmark across all forecast horizons. Additionally, the coefficient α is not significant at $h = 1$, but becomes significant for the medium- and long-term horizons.

[Insert Table 10 here]

Table 10 presents the differences in out-of-sample covariance matrix forecast losses, calculated by comparing the original results from Table 5 with those obtained after replacing the correlation matrix forecasting model with the RM-MHARX setup while keeping the realized variance forecasting models unchanged. These results highlight the improvements in covariance forecasting attributed to the proposed RM-MHAR correlation matrix model. Shaded numbers denote instances where the new forecast losses are lower than the original, while boldface numbers signify whether the differences are statistically significant based on the DM test.

As is shown in Table 10, the RM-MHARX model exhibits superior performance over the MHAR model in nearly all instances with respect to the widely used loss functions: Euclidean and Frobenius, across the three forecast horizons. Moreover, the RM-MHARX model improves the forecast accuracy of MHAR model in terms of QLIKE and Stein losses for medium-term forecasts. These results suggest that introducing the state-level ECI information to forecast the realized correlation of state-level stock returns can further enhance the forecast accuracy of the realized covariance – an expected finding, given the role of the macroeconomic environment in governing comovement in the stock market returns of the US states.

8. Conclusion

In this paper, we introduce the role of low-frequency (weekly) economic conditions indices as predictors to model and forecast the daily RCOV of state-level stocks, derived from 5-minute intraday data, based on the HAR-DRD and the reverse-MIDAS frameworks. Specifically, we first decompose the covariance matrix into a volatility diagonal matrix and a correlation matrix. For the forecasts of univariate volatilities, we combine various HAR-type models with the reverse-MIDAS framework to construct a set of mix-frequency volatility forecasting models that include lower-frequency exogenous predictors involving volatility of the ECIs acting as a proxy for uncertainty. While for the forecasts of the correlation matrix, we adopt the scalar MHAR model that has been widely used in the related literature.

Our findings show that the univariate volatility models which considers the volatility of economic conditions has better in-sample fits. Moreover, the significance level of the coefficient of the volatility of ECI increases as the forecast horizon increases. Second, the out-of-sample forecasting losses indicate that the RM models outperform their benchmark models that do not consider the influence of the second moment of economic conditions. Additionally, the portfolio based on the RM models can generate higher economic gains, such as annualized returns and Sharpe ratios. The Lasso-RM models occasionally also demonstrate excellent performance in the economic evaluation, even though they perform poorly in terms of statistical loss functions. The statistical results continue to hold under various robustness checks involving alternative definitions of the RCOV, dimension of the correlation matrix, alternative measure of the volatility of the ECI, and out-of-sample period. Furthermore, incorporating correlation of ECIs in modeling the realized correlation of stock markets of US states provides greater improvements in the forecasting of the RCOV beyond the case where the volatility of ECI was only considered in the realized variance component. In brief, integrating the reverse-MIDAS modeling framework with the prevailing covariance matrix modeling approach is beneficial for forecasting the covariance matrix, as depicted by our analysis of US state-level stock markets.

Since covariance forecasts serve as key inputs for optimal asset allocation decisions, our findings suggest that incorporating economic uncertainty into forecasting models of realized covariance can enhance portfolio design for investors. Furthermore, given that stock market volatility has historically had negative effects on the U.S. real economy (Pierdzioch and Gupta, 2020; Bouri et al., 2024), policymakers must closely monitor economic uncertainty and tailor the scale and duration of expansionary policies accordingly. This approach helps mitigate the risk of uncertainty-driven covariability in state-level stock markets, preventing it from exacerbating the recessionary effects initially triggered by economic volatility.

Future research avenues could explore extending the reverse-MIDAS framework to incorporate additional sources of macroeconomic uncertainty beyond the volatility of ECIs. Specifically, integrating higher-frequency measures of geopolitical risks, monetary policy uncertainty, and financial market stress indices could enhance the forecasting accuracy of realized covariance matrices. Additionally, given the strong evidence of connectedness among state-level stock returns and economic conditions, network-based econometric approaches such as Graphical VAR or dynamic factor models could be employed to capture the spatial and temporal dependencies across states.

References

Alves, R. P., de Brito, D. S., Medeiros, M. C., & Ribeiro, R. M. (2024). Forecasting Large Realized Covariance Matrices: The Benefits of Factor Models and Shrinkage. Journal of Financial Econometrics, 22(3), 696-742.

Amendola, A., Candila, V., Cipollini, F., & Gallo, G.M. (2024). Doubly multiplicative error models with long- and short-run components. Socio-Economic Planning Sciences, 91, 101764.

Andersen, T. G., Bollerslev, T., & Diebold, F. X. (2007). Roughing it up: Including jump components in the measurement, modeling, and forecasting of return volatility. Review of Economics and Statistics, 89(4), 701--720.

Andersen, T. G., Bollerslev, T., Diebold, F. X., & Labys, P. (2001). The distribution of realized exchange rate volatility. Journal of the American Statistical Association, 96(453), 42–55.

Andersen, T. G., Bollerslev, T., Diebold, F. X., & Labys, P. (2003). Modeling and Forecasting Realized Volatility. Econometrica, 71(2), 579-625.

Archakov, I., & Hansen, P. R. (2021). A New Parametrization of Correlation Matrices. Econometrica, 89(4), 1699-1715.

Archakov, I., Hansen, P. R., & Lunde, A. (2024). A Multivariate Realized GARCH Model. arXiv preprint arXiv:2012.02708.

Arias, J. E., Rubio-Ramírez, J. F., & Shin, M. (2023). Macroeconomic forecasting and variable ordering in multivariate stochastic volatility models. Journal of Econometrics, 235(2), 1054–1086.

Asai, M., Gupta, R., & McAleer, M. (2020). Forecasting volatility and co-volatility of crude oil and gold futures: Effects of leverage, jumps, spillovers, and geopolitical risks. International Journal of Forecasting, 36(3), 933-948.

Barndorff-Nielsen, O. E., Hansen, P. R., Lunde, A., & Shephard, N. (2011). Multivariate realised kernels: Consistent positive semi-definite estimators of the covariation of equity prices with noise and non-synchronous trading. Journal of Econometrics, 162(2), 149-169.

Barndorff-Nielsen, O. E., Kinnebrouk, S., & Shephard, N. (2010). Measuring downside risk: Realised semivariance. In Volatility and Time Series Econometrics: Essays in Honor of Robert F. Engle ((Edited by T. Bollerslev, J. Russell and M. Watson), pp. 117-136). Oxford University Press.

Barndorff-Nielsen, O. E., & Shephard, N. (2004). Power and bipower variation with stochastic volatility and jumps. Journal of Financial Econometrics, 2(1), 1-37.

Bauer, G. H., & Vorkink, K. (2011). Forecasting multivariate realized stock market volatility. Journal of Econometrics, 160(1), 93-101.

Bauwens, L., Laurent, S., & Rombouts, J. V. K. (2006). Multivariate GARCH models: A survey. Journal of Applied Econometrics, 21(1), 79-109.

Bauwens, L., & Otranto, E. (2023). Modeling Realized Covariance Matrices: A Class of Hadamard Exponential Models. Journal of Financial Econometrics, 21(4), 1376-1401.

Bernanke, B. S. (1983). Irreversibility, uncertainty, and cyclical investment. Quarterly Journal of Economics, 98(1), 85-106.

Bollerslev, T., Patton, A. J., & Quaedvlieg, R. (2018). Modeling and forecasting (un)reliable realized covariances for more reliable financial decisions. Journal of Econometrics, 207(1), 71-91.

Bouri, E., Gupta, R., Pierdzioch, C., & Polat, O. (2024). Forecasting U.S. recessions using over 150 years of data: Stock-market moments versus oil-market moments. Finance Research Letters, 69 (Part B), 106179.

Callot, L. A. F., Kock, A. B., & Medeiros, M. C. (2017). Modeling and forecasting large realized

covariance matrices and portfolio choice. Journal of Applied Econometrics, 32(1), 140-158.
Caporin, M., Rossi, E., & Santucci de Magistris, P. (2016). Volatility jumps and their economic determinants. Journal of Financial Econometrics, 14(1), 29-80.
Cepni, O., Gupta, R., Liao, W., & Ma, J. (2024). Climate risks and forecastability of the weekly state-level economic conditions of the United States. International Review of Finance, 24(1), 154-162.
Chaney, T., Sraer, D., & Thesmar, D. (2012). The collateral channel: how real estate shocks affect corporate investment. American Economic Review, 102(6), 2381-2409.
Chiriac, R., & Voev, V. (2011). Modelling and forecasting multivariate realized volatility. Journal of Applied Econometrics, 26(6), 922-947.
Corsi, F. (2009). A simple approximate Long-memory model of realized volatility. Journal of Financial Econometrics, 7(2), 174-196.
Coval, J. D., & Moskowitz, T. J. (1999). Home bias at home: local equity preference in domestic portfolios. Journal of Finance, 54(6), 2045-2073.
Coval, J. D., & Moskowitz, T. J. (2001). The geography of investment: Informed trading and asset prices. Journal of Political Economy, 199(4), 811-841.
DeMiguel, V., Garlappi, L., Nogales, F. J., & Uppal, R. (2009). A Generalized Approach to Portfolio Optimization: Improving Performance by Constraining Portfolio Norms. Management Science.
Diebold, F. X., & Mariano, R. S. (1995). Comparing predictive accuracy. Journal of Business & Economic Statistics, 13(3), 253-263.
Engle, R. (2002). Dynamic Conditional Correlation: A Simple Class of Multivariate Generalized Autoregressive Conditional Heteroskedasticity Models. Journal of Business & Economic Statistics, 20(3), 339-350.
Engle, R. F., Ghysels, E., & Sohn, B. (2013). Stock Market Volatility and Macroeconomic Fundamentals. Review of Economics and Statistics, 95(3), 776–797.
Fleming, J., Kirby, C., & Ostdiek, B. (2001). The Economic Value of Volatility Timing. The Journal of Finance, 56(1), 329-352.
Fleming, J., Kirby, C., & Ostdiek, B. (2003). The economic value of volatility timing using “realized” volatility. Journal of Financial Economics, 67(3), 473-509.
Foroni, C., Guérin, P., & Marcellino, M. (2018). Using low frequency information for predicting high frequency variables. International Journal of Forecasting, 34(4), 774-787.
Foroni, C., Ravazzolo, F., & Rossini, L. (2023). Are low frequency macroeconomic variables important for high frequency electricity prices? Economic Modelling, 120, 106160.
Friedman, J., Hastie, T., & Tibshirani, R. (2010). Regularization Paths for Generalized Linear Models via Coordinate Descent. Journal of Statistical Software, 33(1), 1-22.
Goyal, A., Welsch, I., & Zafirov, A. (2024). A Comprehensive 2022 Look at the Empirical Performance of Equity Premium Prediction. Review of Financial Studies 37(11), 3490-3557.
Gribisch, B., & Hartkopf, J. P. (2023). Modeling realized covariance measures with heterogeneous liquidity: A generalized matrix-variate Wishart state-space model. Journal of Econometrics, 235(1), 43-64.
Gunnarsson, E. S., Isern, H. R., Kaloudis, A., Risstad, M., Vigdel, B., & Westgaard, S. (2024). Prediction of realized volatility and implied volatility indices using AI and machine learning: A review. International Review of Financial Analysis, 93, 103221.
Hafner, C. M., & Wang, L. (2023). A dynamic conditional score model for the log correlation matrix.

Journal of Econometrics, 237(2), 105176.
Hansen, P. R., Lunde, A., & Nason, J. M. (2011). The model confidence set. Econometrica, 79(2), 453-497.
Harvey, A., Ruiz, E., & Shephard, N. (1994). Multivariate Stochastic Variance Models. The Review of Economic Studies, 61(2), 247-264.
Hecq, A., Ternes, M., & Wilms, I. (2024). Hierarchical Regularizers for Reverse Unrestricted Mixed Data Sampling Regressions. arXiv preprint arXiv:2301.10592.
Huang, X., & Tauchen, G. (2005). The Relative Contribution of Jumps to Total Price Variance. Journal of Financial Econometrics, 3(4), 456-499.
Jagannathan, R., & Ma, T. (2003). Risk Reduction in Large Portfolios: Why Imposing the Wrong Constraints Helps. The Journal of Finance, 58(4), 1651-1683.
Korniotis, G. M., & Kumar, A. (2013). State-level business cycles and local return predictability. Journal of Finance, 68(3), 1037-1096.
Laurent, S., Rombouts, J. V. K., & Violante, F. (2012). On the forecasting accuracy of multivariate GARCH models. Journal of Applied Econometrics, 27(6), 934-955.
Li, D., Drovandi, C., & Clements, A. (2024). Outlier-robust methods for forecasting realized covariance matrices. International Journal of Forecasting, 40(1), 392-408.
Luo, J., Cepni, O., Demirer, R., & Gupta, R. (Forthcoming). Forecasting Multivariate Volatilities with Exogenous Predictors: An Application to Industry Diversification Strategies. Journal of Empirical Finance.
Luo, J., & Chen, L. (2020). Realized volatility forecast with the Bayesian random compressed multivariate HAR model. International Journal of Forecasting, 36(3), 781-799.
Luo, J., Klein, T., Ji, Q., & Hou, C. (2022). Forecasting realized volatility of agricultural commodity futures with infinite Hidden Markov HAR models. International Journal of Forecasting, 38(1), 51-73.
Marcellino, M., Stock, J. H., & Watson, M. W. (2006). A comparison of direct and iterated multistep AR methods for forecasting macroeconomic time series. Journal of Econometrics, 135(1), 499-526.
McAleer, M., & Medeiros, M.C. (2008). Realized volatility: A review. Econometric Reviews, 27(1-3), 10-45.
Oh, D. H., & Patton, A. J. (2016). High-dimensional copula-based distributions with mixed frequency data. Journal of Econometrics, 193(2), 349-366.
Opschoor, A., Janus, P., Lucas, A., & Van Dijk, D. (2018). New HEAVY Models for Fat-Tailed Realized Covariances and Returns. Journal of Business & Economic Statistics, 36(4), 643-657.
Opschoor, A., Lucas, A., & Rossini, L. (2024). The Conditional Autoregressive F -Riesz Model for Realized Covariance Matrices. Journal of Financial Econometrics, nbae023.
Pakel, C., Shephard, N., Sheppard, K., & Engle, R. F. (2021). Fitting Vast Dimensional Time-Varying Covariance Models. Journal of Business & Economic Statistics, 39(3), 652-668.
Patton, A. J., & Sheppard, K. (2015). Good volatility, bad volatility: Signed jumps and the persistence of volatility. The Review of Economics and Statistics, 97(3), 683-697.
Pierdzioch, C., & Gupta, R. (2020). Uncertainty and forecasts of U.S. recessions. Studies in Nonlinear Dynamics and Econometrics, 24(4), 1-20.
Pirinsky, C., & Wang, Q. (2006). Does corporate headquarters location matter for stock returns? Journal of Finance, 61, 1991-2015.
Polat, O., Cunado, J., Cepni, O., & Gupta, R. (2024). Oil price shocks and the connectedness of US

state-level financial markets. Energy Economics, 141, 108128.
Salisu, A. A., Liao, W., Gupta, R., & Cepni, O. (2025). Economic Conditions and Predictability of US Stock Returns Volatility: Local Factor Versus National Factor in a GARCH-MIDAS Model. Journal of Forecasting.
Schwert, G. W. (1989). Why does stock market volatility change over time? Journal of Finance, 44(5), 1115-1153.
Segnon, M., Gupta, R., & Wilfling, B. (2024). Forecasting stock market volatility with regimes-witching GARCH-MIDAS: the role of geopolitical risks. International Journal of Forecasting, 40(1), 29-43.
Sévi, B. (2014). Forecasting the volatility of crude oil futures using intraday data. European Journal of Operational Research, 235(3), 643-659.
Shiller, R. J. (1981a). Do stock prices move too much to be justified by subsequent changes in dividends? American Economic Review, 71(3), 421-436.
Shiller, R. J. (l981b). The use of volatility measures in assessing market efficiency. Journal of Finance, 36(2), 291-304.
Symitsi, E., Symeonidis, L., Kourtis, A., & Markellos, R. (2018). Covariance forecasting in equity markets. Journal of Banking & Finance, 96, 153-168.
Tibshirani, R. (1996). Regression shrinkage and selection via the lasso. Journal of the Royal Statistical Society: Series B (Methodological), 58(1), 267-288.
Vassallo, D., Buccheri, G., & Corsi, F. (2021). A DCC-type approach for realized covariance modeling with score-driven dynamics. International Journal of Forecasting, 37(2), 569-586.
Wilms, I., Rombouts, J., & Croux, C. (2021). Multivariate volatility forecasts for stock market indices. International Journal of Forecasting, 37(2), 484-499.
Zhang, C., Pu, X., Cucuringu, M., & Dong, X. (2024). Graph-based methods for forecasting realized covariances. Journal of Financial Econometrics. DOI: https://doi.org/10.1093/jjfinec/nbae026..

Table 1. Description of realized covariance matrix forecasting models

Covariance models	Univariate variance models	Correlation matrix models	Exogenous variables
Group 1:			
HAR-DRD	HAR		None
RM-HARX-DRD	RM-HARX		The log volatility of the corresponding state's ECI
PCA-HARX-DRD	PCA-HARX		The first PCA component extracted from log volatilities for all fifty states' ECIs
Lasso-RM-HARX-DRD	Lasso-RM-HARX		The log volatilities for all fifty states' ECIs
Group 2:			
HARJ-DRD	HARJ		None
RM-HARJX-DRD	RM-HARJX		The log volatility of the corresponding state's ECI
PCA-RM-HARJX-DRD	PCA-RM-HARJX		The first PCA component extracted from log volatilities for all fifty states' ECIs
Lasso-RM-HARJX-DRD	Lasso-RM-HARJX	Scalar MHAR (or scalar RM-MHARX in Section 7)	The log volatilities for all fifty states' ECIs
Group 3:			
HARCJ-DRD	HARCJ		None
RM-HARCJX-DRD	RM-HARCJX		The log volatility of the corresponding state's ECI
PCA-RM-HARCJX-DRD	PCA-RM-HARCJX		The first PCA component extracted from log volatilities for all fifty states' ECIs
Lasso-RM-HARCJX-DRD	Lasso-RM-HARCJX		The log volatilities for all fifty states' ECIs
Group 4:			
HARRS-DRD	HARRS		None
RM-HARRSX-DRD	RM-HARRSX		The log volatility of the corresponding state's ECI
PCA-RM-HARRSX-DRD	PCA-RM-HARRSX		The first PCA component extracted from log volatilities for all fifty states' ECIs
Lasso-RM-HARRSX-DRD	Lasso-RM-HARRSX		The log volatilities for all fifty states' ECIs

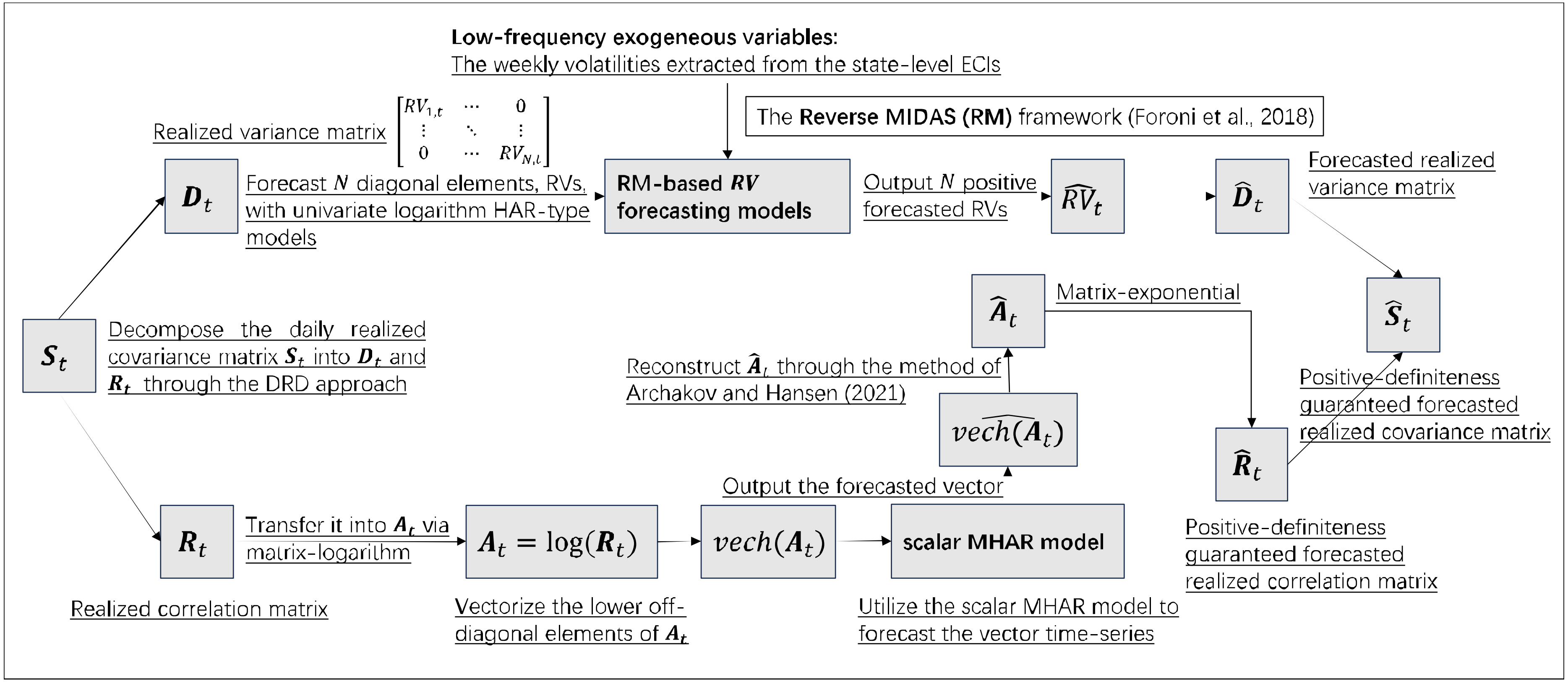

Figure 1. Forecasting procedure description

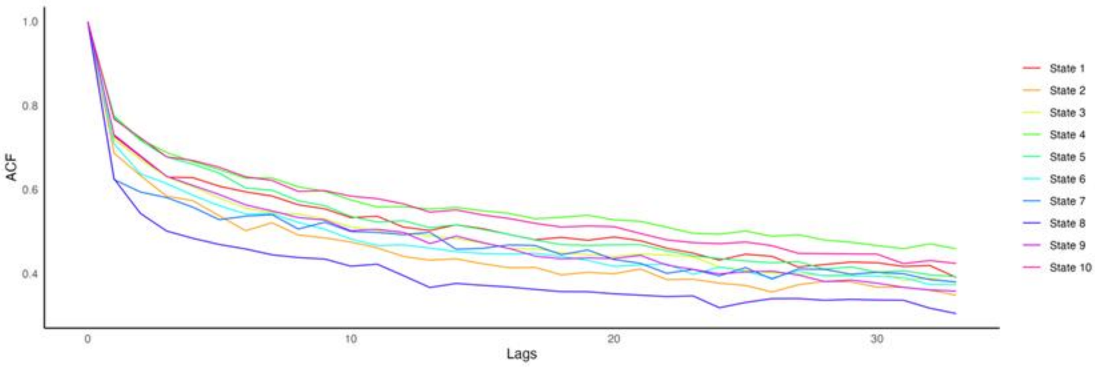

Figure 2. The autocorrelation function of log realized variances for selected ten states

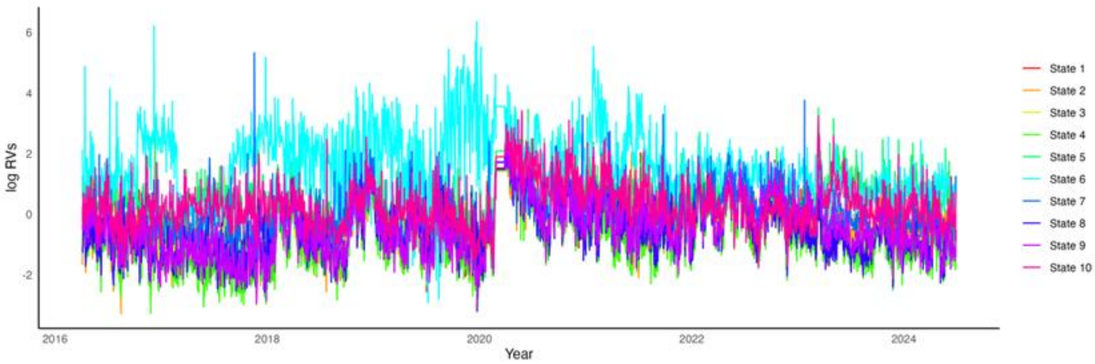

(a) log RVs (daily)

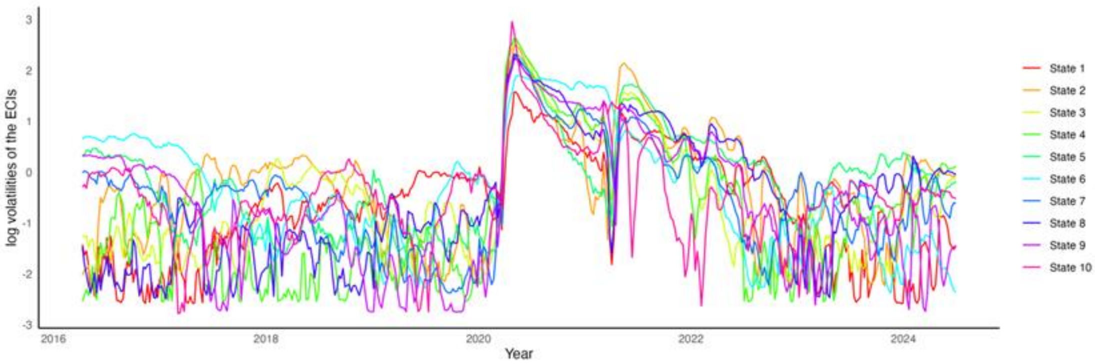

(b) log volatilities of the ECIs (weekly)

Figure 3. Data plot

Table 2. In-sample estimates (h=1)

	HAR(X)		HARJ(X)		HARCJ(X)		HARRS(X)	
	Standard	RM	Standard	RM	Standard	RM	Standard	RM
β_d	0.354	0.358	0.427	0.434	0.348	0.354	0.175	0.178
	(0.025)	(0.057)	(0.028)	(0.064)	(0.026)	(0.059)	(0.023)	(0.053)
β_w	0.280	0.279	0.263	0.260	0.292	0.287	0.080	0.082
	(0.040)	(0.090)	(0.040)	(0.090)	(0.042)	(0.095)	(0.042)	(0.094)
β_m	0.263	0.246	0.268	0.247	0.186	0.176	0.096	0.077
	(0.035)	(0.082)	(0.035)	(0.082)	(0.038)	(0.086)	(0.057)	(0.128)
γ_d			-0.308	-0.333	0.085	0.080	0.196	0.199
			(0.052)	(0.121)	(0.052)	(0.121)	(0.022)	(0.049)
γ_w					-0.097	-0.094	0.182	0.178
					(0.093)	(0.210)	(0.042)	(0.093)
γ_m					0.383	0.327	0.170	0.166
					(0.100)	(0.232)	(0.061)	(0.136)
α		0.020		0.026		0.025		0.027
		(0.027)		(0.028)		(0.029)		(0.028)
Adj. R^2	0.580	0.583	0.587	0.591	0.594	0.599	0.592	0.596

Note: The table reports the in-sample parameter estimates, standard errors (in parentheses) and adjusted R^2 for different models. Following Bollerslev et al. (2018), all results represented are the averages across the ten randomly selected state-level stock market indices.

Table 3. In-sample estimates (h=5)

	HAR(X)		HARJ(X)		HARCJ(X)		HARRS(X)	
	Standard	RM	Standard	RM	Standard	RM	Standard	RM
β_d	0.247	0.250	0.297	0.307	0.249	0.256	0.113	0.116
	(0.021)	(0.047)	(0.023)	(0.053)	(0.022)	(0.049)	(0.019)	(0.043)
β_w	0.242	0.241	0.228	0.225	0.251	0.244	0.039	0.040
	(0.033)	(0.074)	(0.033)	(0.074)	(0.035)	(0.078)	(0.034)	(0.077)
β_m	0.361	0.328	0.362	0.325	0.247	0.230	0.174	0.144
	(0.029)	(0.068)	(0.029)	(0.067)	(0.031)	(0.071)	(0.046)	(0.105)
γ_d			-0.224	-0.257	0.010	-0.002	0.138	0.141
			(0.043)	(0.101)	(0.043)	(0.100)	(0.018)	(0.040)
γ_w					-0.027	-0.008	0.198	0.193
					(0.077)	(0.174)	(0.034)	(0.076)
γ_m					0.469	0.373	0.190	0.185
					(0.083)	(0.193)	(0.050)	(0.111)
α		0.038		0.045		0.043		0.043
		(0.023)		(0.023)		(0.024)		(0.023)
Adj. R^2	0.632	0.634	0.638	0.641	0.647	0.650	0.647	0.649

Note: The table reports the in-sample parameter estimates, standard errors (in parentheses) and adjusted R^2 for different models. Following Bollerslev et al. (2018), all results represented are the averages across the ten randomly selected state-level stock market indices.

Table 4. In-sample estimates (*h*=20)

	HAR(X)		HARJ(X)		HARCJ(X)		HARRS(X)	
	Standard	RM	Standard	RM	Standard	RM	Standard	RM
β_d	0.147	0.149	0.160	0.169	0.149	0.153	0.060	0.061
	(0.021)	(0.046)	(0.023)	(0.052)	(0.021)	(0.048)	(0.019)	(0.042)
β_w	0.173	0.174	0.167	0.165	0.169	0.162	0.013	0.014
	(0.032)	(0.073)	(0.032)	(0.073)	(0.034)	(0.077)	(0.034)	(0.075)
β_m	0.429	0.379	0.426	0.374	0.315	0.292	0.370	0.329
	(0.029)	(0.066)	(0.029)	(0.066)	(0.031)	(0.069)	(0.045)	(0.102)
γ_d			-0.070	-0.100	0.018	0.019	0.089	0.090
			(0.043)	(0.099)	(0.042)	(0.099)	(0.017)	(0.039)
γ_w					0.045	0.064	0.171	0.168
					(0.076)	(0.172)	(0.033)	(0.075)
γ_m					0.421	0.266	0.045	0.040
					(0.082)	(0.190)	(0.049)	(0.109)
α		0.059		0.065		0.067		0.059
		(0.022)		(0.023)		(0.023)		(0.022)
Adj. R^2	0.576	0.583	0.578	0.586	0.588	0.596	0.594	0.600

Note: The table reports the in-sample parameter estimates, standard errors (in parentheses) and adjusted R^2 for different models. Following Bollerslev et al. (2018), all results represented are the averages across the ten randomly selected state-level stock market indices.

Table 5. Out-of-sample forecasting losses

	Short horizon (*h*=1)				Medium horizon (*h*=5)				Long horizon (*h*=20)			
	L^{Eucl}	L^{Frob}	L^{QLIKE}	L^{Stein}	L^{Eucl}	L^{Frob}	L^{QLIKE}	L^{Stein}	L^{Eucl}	L^{Frob}	L^{QLIKE}	L^{Stein}
Group 1:												
HAR-DRD	**4.432**	5.373	5.782	3.284	**3.624**	4.324	**5.850**	**1.583**	3.503	4.167	**6.119**	**1.088**
RM-HARX-DRD	**4.435**	5.378	**5.773***	**3.275***	**3.612***	**4.310***	**5.842***	**1.575***	**3.480***	**4.142***	**6.120**	**1.088**
PCA-RM-HARX-DRD	**4.420***	**5.361***	**5.773***	**3.275***	**3.612***	**4.304***	**5.844***	**1.577***	3.521	4.172	**6.133**	1.101
Lasso-RM-HARX-DRD	4.453	5.393	5.819	3.321	3.707	4.405	6.003	1.736	5.444	6.266	7.602	2.571
Group 2:												
HARJ-DRD	**4.417**	**5.352**	5.776	**3.278**	3.637	4.344	5.867	1.600	**3.463**	**4.140**	**6.127**	**1.095**
RM-HARJX-DRD	**4.413**	**5.349***	**5.765***	**3.267***	**3.614***	**4.317***	**5.857***	**1.590***	**3.413***	**4.096***	**6.125***	**1.093***
PCA-RM-HARJX-DRD	**4.405***	**5.339***	**5.763***	**3.265***	**3.604***	**4.299***	**5.855***	**1.587***	**3.449***	**4.113***	**6.131**	1.100
Lasso-RM-HARJX-DRD	**4.429**	**5.364**	5.817	3.319	3.680	4.380	5.997	1.730	5.422	6.247	7.586	2.555
Group 3:												
HARCJ-DRD	4.533	5.463	5.799	3.301	3.750	4.452	5.887	1.620	3.559	4.232	6.163	1.131
RM-HARCJX-DRD	4.526	5.457*	5.779*	**3.281***	3.720*	4.427*	5.874*	1.607*	**3.486***	4.179*	6.160*	1.128*
PCA-RM-HARCJX-DRD	4.505*	5.435*	**5.756***	**3.258***	3.696*	4.394*	**5.855***	**1.588***	**3.484***	**4.155***	**6.140***	**1.108***
Lasso-RM-HARCJX-DRD	4.529*	5.457*	5.810	3.312	3.709*	4.407*	5.957	1.690	5.307	6.111	7.574	2.543
Group 4:												
HARRS-DRD	4.456	5.394	5.793	3.295	3.644	4.345	**5.854**	**1.587**	3.530	4.189	**6.149**	1.117
RM-HARRSX-DRD	4.459	5.397	5.780*	**3.282***	**3.628***	4.325*	**5.844***	**1.577***	3.505*	**4.162***	**6.147***	1.115*
PCA-RM-HARRSX-DRD	**4.444***	5.380*	5.778*	**3.280***	**3.628***	**4.319***	**5.845***	**1.577***	3.546	4.191	6.155	1.123
Lasso-RM-HARRSX-DRD	4.475	5.410	5.819	3.321	3.701	4.395	5.961	1.694	5.338	6.144	7.508	2.476

Note: The table reports out-of-sample forecast loss for the five groups of models. Entries in boldface indicate models that are part of the 75% model confidence set (MCS) for all models across the relevant loss. For each group, RM models that significantly improve on their non-RM benchmark model via DM test are indicated by an asterisk.

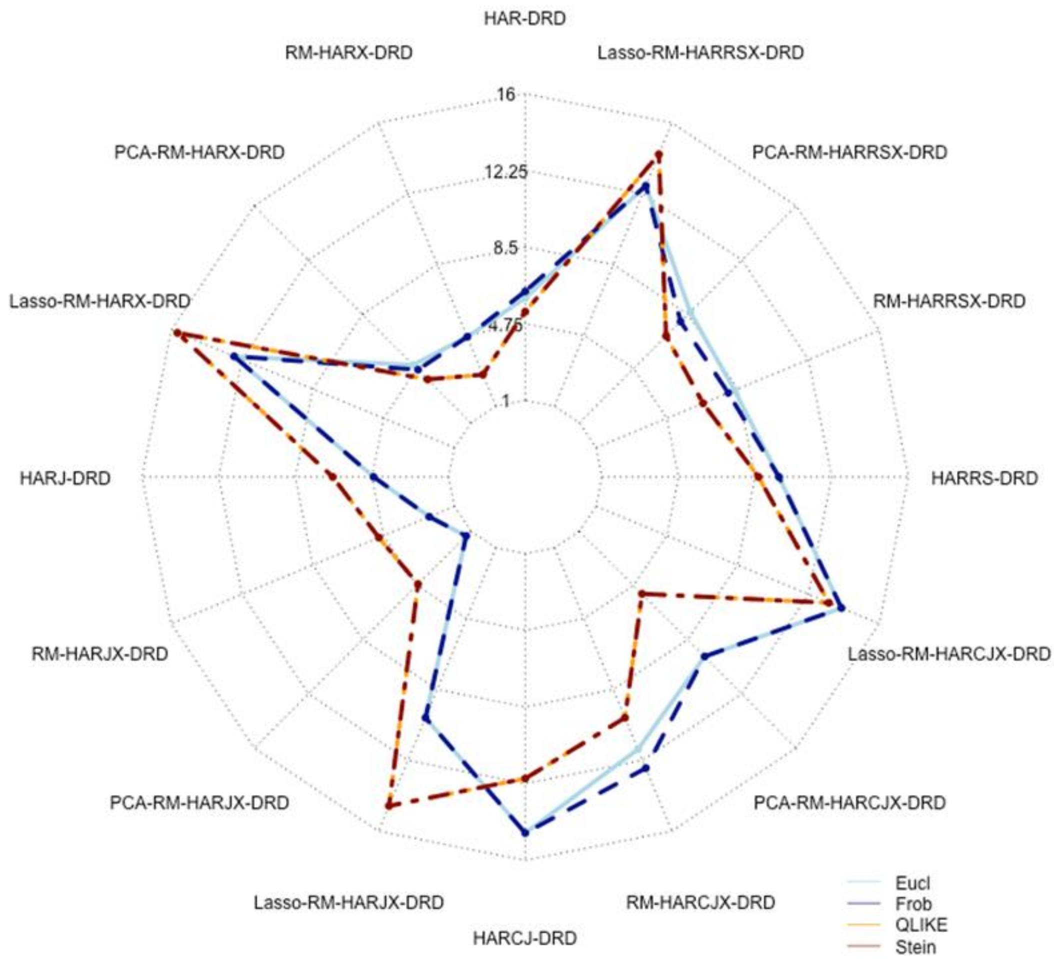

Figure 4. Model rankings based on different loss functions

Note: Each colored line shows the relative rankings of models for the corresponding loss functions. The model rankings are averaged across the three kinds of forecast horizons. Lower rankings indicate better performance, thus the closer a model is to the center of the graph, the better it is.

Table 6. Portfolio performance for short horizon (h=1)

	$Annualized$ $Return$	Economic value (%) $\gamma = 1$	$\gamma = 10$	σ_p(%)	$Sharp$(%)	CO	SP
Group 1:							
HAR-DRD	5.910	-	-	**0.876**	2.601	**0.765**	-0.326
RM-HARX-DRD	6.297	0.362	0.332	0.878	2.761	0.770	-0.332
PCA-RM-HARX-DRD	5.544	-0.349	-0.375	0.878	2.440	0.767	-0.325
Lasso-RM-HARX-DRD	5.877	-0.040	-0.119	0.880	2.575	0.772	-0.327
Group 2:							
HARJ-DRD	5.642	-	-	0.885	2.462	0.781	-0.335
RM-HARJX-DRD	6.232	0.548	0.447	0.890	2.697	0.785	-0.339
PCA-RM-HARJX-DRD	5.418	-0.216	-0.256	0.887	2.362	0.783	-0.334
Lasso-RM-HARJX-DRD	4.851	-0.753	-0.787	0.886	2.121	0.787	-0.336
Group 3:							
HARCJ-DRD	7.207	-	-	0.881	3.136	0.780	-0.325
RM-HARCJX-DRD	**8.137**	0.852	0.714	0.888	**3.498**	0.778	-0.327
PCA-RM-HARCJX-DRD	6.976	-0.221	-0.274	0.883	3.029	0.777	**-0.324**
Lasso-RM-HARCJX-DRD	7.208	-0.006	-0.075	0.884	3.124	0.785	-0.326
Group 4:							
HARRS-DRD	4.904	-	-	0.879	2.161	0.767	-0.328
RM-HARRSX-DRD	5.370	0.439	0.396	0.881	2.355	0.769	-0.331
PCA-RM-HARRSX-DRD	4.649	-0.244	-0.251	0.880	2.050	0.767	-0.325
Lasso-RM-HARRSX-DRD	3.940	-0.929	-1.021	0.884	1.735	0.770	-0.328

Note: The table reports portfolio performance for the different models. Entries in shade indicate models that outperform their benchmarks for the relevant column, and entries in boldface indicate the best models for the relevant column.

Table 7. Portfolio performance for medium horizon (h=5)

	$Annualized$ $Return$	Economic value (%) $\gamma = 1$	Economic value (%) $\gamma = 10$	$\sigma_p(\%)$	$Sharp(\%)$	CO	SP
Group 1:							
HAR-DRD	7.571	-	-	0.876	3.307	0.728	-0.284
RM-HARX-DRD	8.053	0.440	0.357	0.880	3.494	0.730	-0.283
PCA-RM-HARX-DRD	7.397	-0.163	-0.176	0.877	3.231	**0.725**	-0.275
Lasso-RM-HARX-DRD	9.809	2.037	1.635	0.895	4.148	0.742	-0.288
Group 2:							
HARJ-DRD	7.585	-	-	0.875	3.315	0.738	-0.293
RM-HARJX-DRD	8.409	0.756	0.663	0.880	3.642	0.741	-0.291
PCA-RM-HARJX-DRD	7.371	-0.199	-0.200	0.876	3.224	0.737	-0.284
Lasso-RM-HARJX-DRD	9.516	1.762	1.465	0.890	4.055	0.746	-0.294
Group 3:							
HARCJ-DRD	8.847	-	-	0.861	3.910	0.752	-0.283
RM-HARCJX-DRD	9.861	0.917	0.788	0.867	4.305	0.750	-0.285
PCA-RM-HARCJX-DRD	8.590	-0.238	-0.251	**0.861**	3.797	0.749	-0.279
Lasso-RM-HARCJX-DRD	**10.086**	1.100	0.756	0.878	**4.345**	0.760	-0.297
Group 4:							
HARRS-DRD	7.143	-	-	0.873	3.135	0.730	-0.284
RM-HARRSX-DRD	7.806	0.610	0.535	0.877	3.401	0.730	-0.281
PCA-RM-HARRSX-DRD	6.971	-0.161	-0.161	0.874	3.062	0.727	**-0.274**
Lasso-RM-HARRSX-DRD	8.150	0.920	0.744	0.882	3.525	0.742	-0.289

Note: The table reports portfolio performance for the different models. Entries in shade indicate models that outperform their benchmarks for the relevant column, and entries in boldface indicate the best models for the relevant column.

Table 8. Portfolio performance for long horizon (h=20)

	$Annualized$ $Return$	Economic value (%)		σ_p(%)	$Sharp$(%)	CO	SP
		$\gamma = 1$	$\gamma = 10$				
Group 1:							
HAR-DRD	9.296	-	-	0.891	3.959	0.718	-0.267
RM-HARX-DRD	9.878	0.520	0.409	0.896	4.172	0.724	-0.258
PCA-RM-HARX-DRD	9.118	-0.163	-0.152	0.890	3.889	**0.712**	**-0.246**
Lasso-RM-HARX-DRD	8.136	-1.207	-2.509	0.954	3.253	0.737	-0.296
Group 2:							
HARJ-DRD	9.901	-	-	0.891	4.207	0.742	-0.274
RM-HARJX-DRD	**10.452**	0.489	0.372	0.896	**4.402**	0.750	-0.271
PCA-RM-HARJX-DRD	9.673	-0.206	-0.195	0.890	4.118	0.740	-0.257
Lasso-RM-HARJX-DRD	7.244	-2.596	-4.197	0.969	2.865	0.737	-0.296
Group 3:							
HARCJ-DRD	9.536	-	-	0.884	4.090	0.791	-0.279
RM-HARCJX-DRD	10.340	0.715	0.540	0.892	4.377	0.788	-0.286
PCA-RM-HARCJX-DRD	9.712	0.164	0.190	**0.882**	4.169	0.792	-0.275
Lasso-RM-HARCJX-DRD	7.861	-1.731	-3.537	0.972	3.092	0.790	-0.314
Group 4:							
HARRS-DRD	9.621	-	-	0.897	4.064	0.739	-0.269
RM-HARRSX-DRD	10.186	0.502	0.383	0.903	4.264	0.744	-0.262
PCA-RM-HARRSX-DRD	9.317	-0.276	-0.261	0.896	3.945	0.736	-0.249
Lasso-RM-HARRSX-DRD	7.226	-2.317	-3.491	0.954	2.901	0.741	-0.303

Note: The table reports portfolio performance for the different models. Entries in shade indicate models that outperform their benchmarks for the relevant column, and entries in boldface indicate the best models for the relevant column.

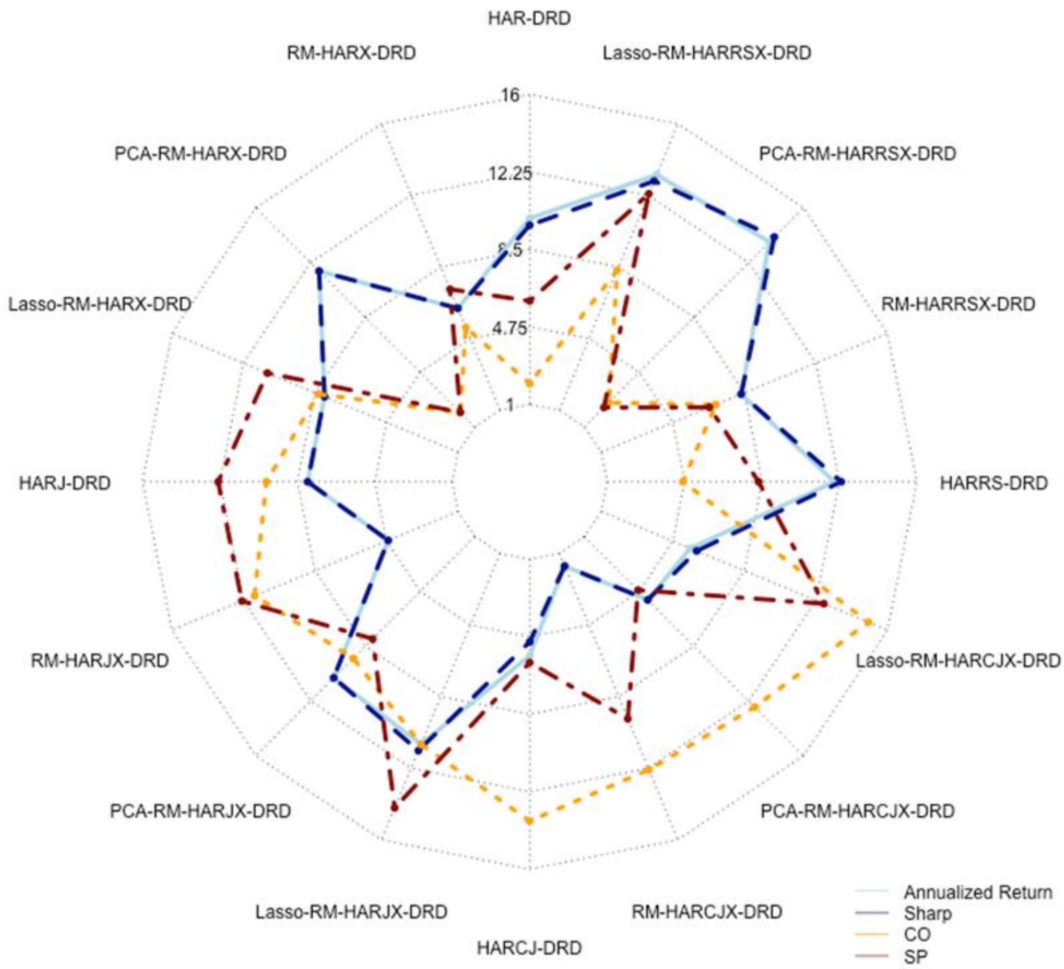

Figure 5. Model rankings based on different economic evaluation metrics

Note: Each colored line shows the relative rankings of models for the corresponding economic evaluation criteria. The model rankings are averaged across the three kinds of forecast horizons. Lower rankings indicate better performance, thus the closer a model is to the center of the graph, the better it is.

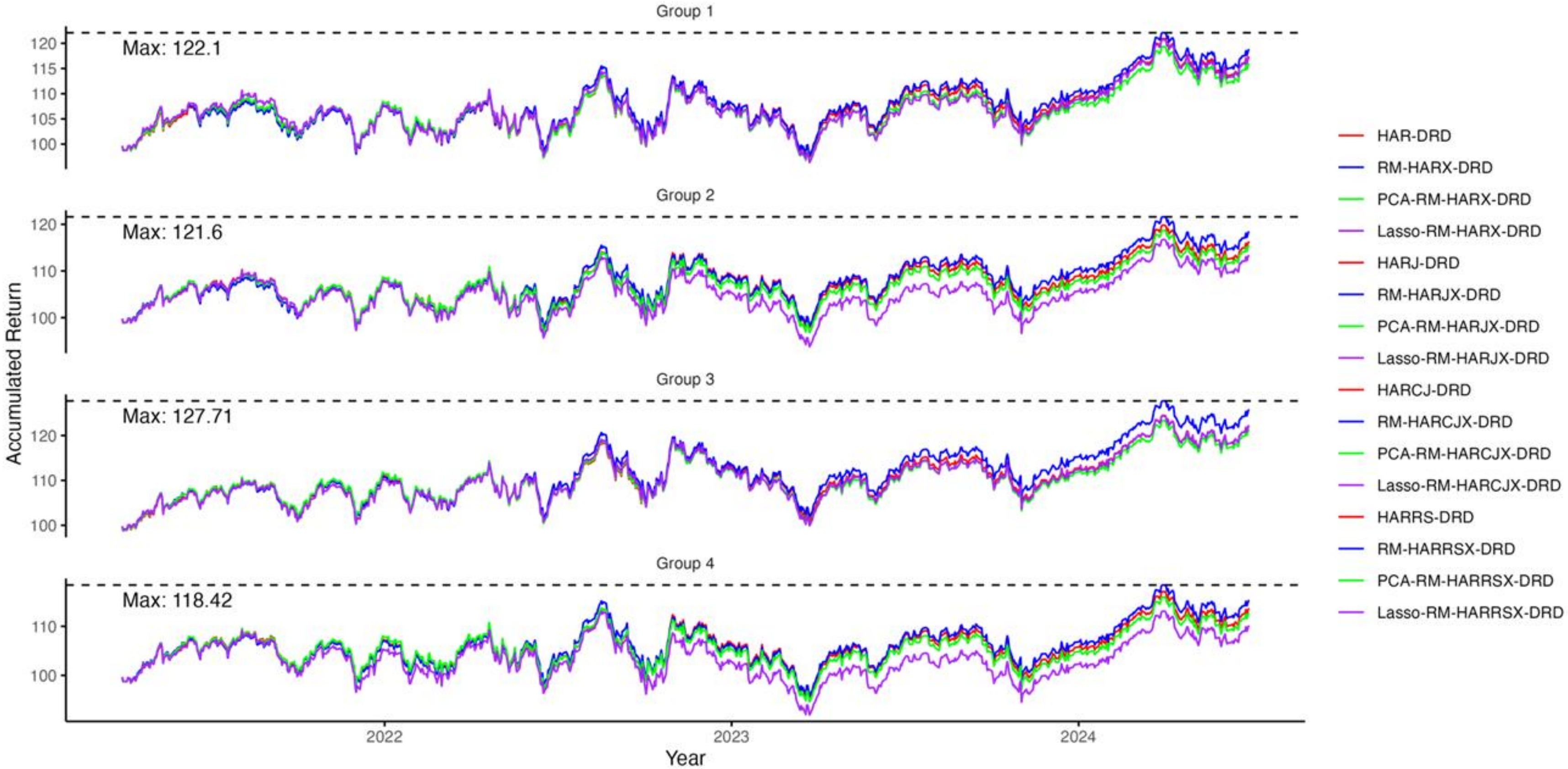

Figure 6. Accumulated return for short horizon (*h*=1)

Note: All models of the same type in the groups are represented by lines of the same color. For instance, the four kinds of PCA-RM models in all groups are indicated in green.

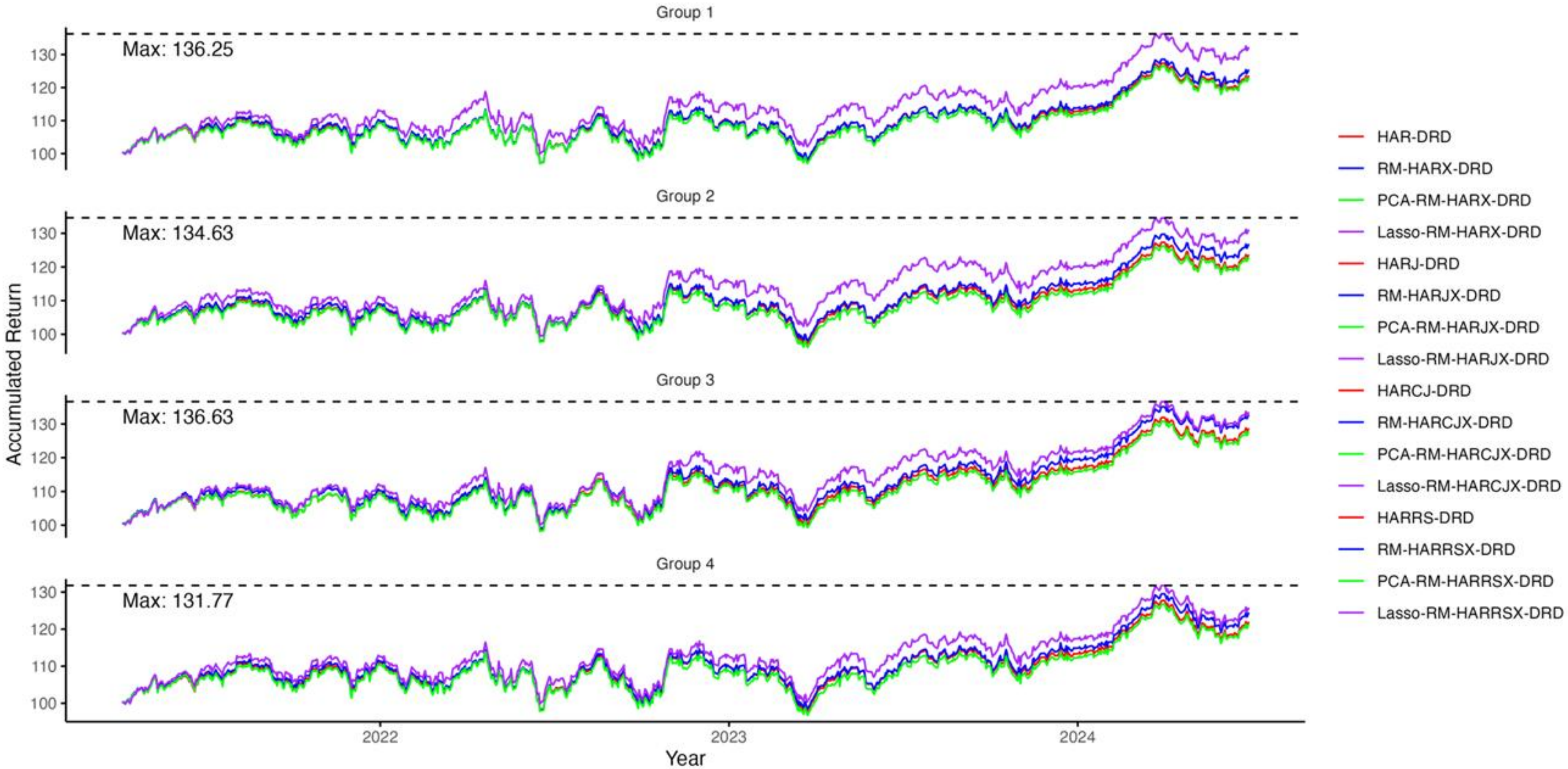

Figure 7. Accumulated return for medium horizon (h=5)

Note: All models of the same type in the groups are represented by lines of the same color. For instance, the four kinds of PCA-RM models in all groups are indicated in green.

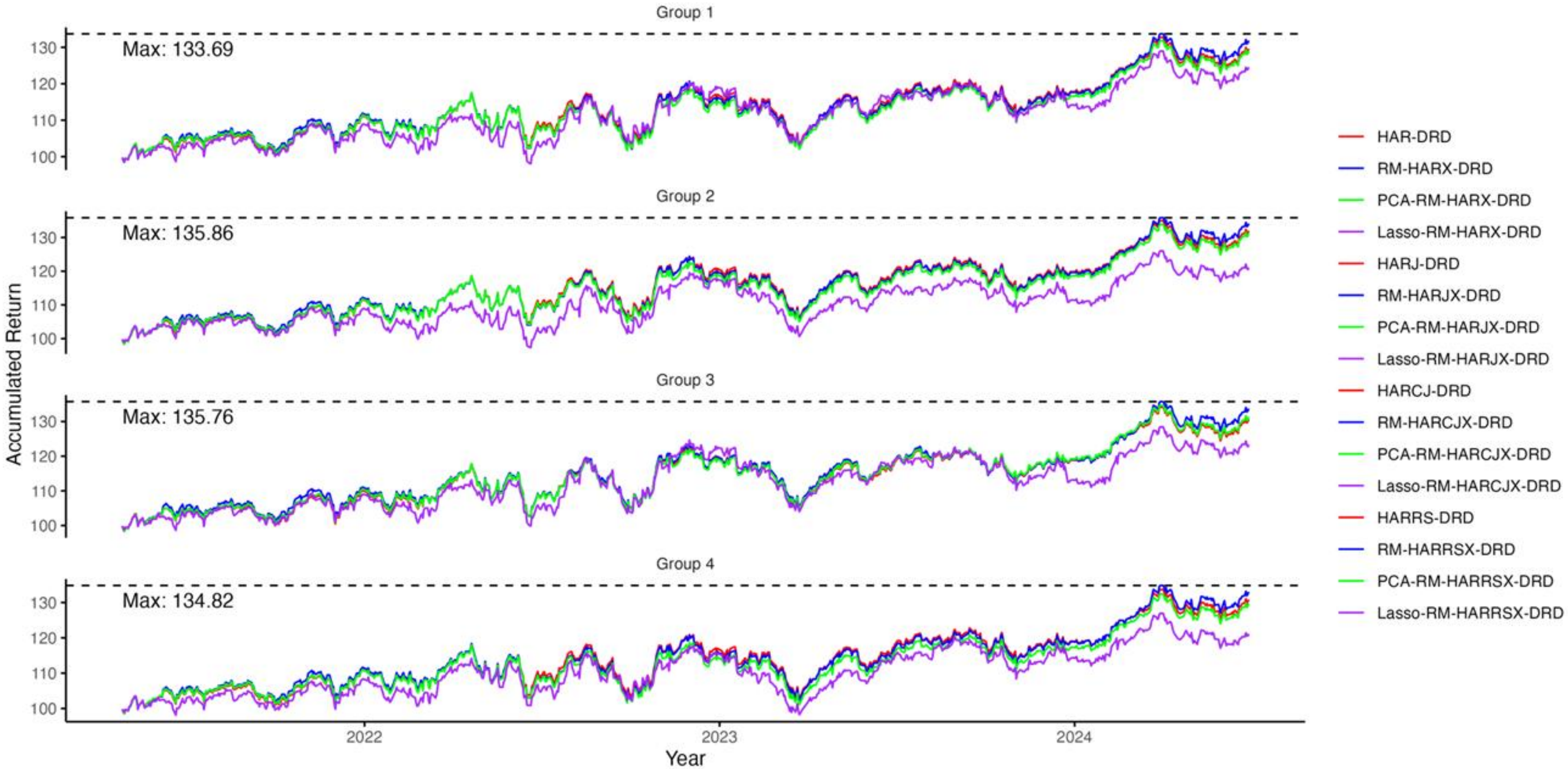

Figure 8. Accumulated return for long horizon (*h*=20)

Note: All models of the same type in the groups are represented by lines of the same color. For instance, the four kinds of PCA-RM models in all groups are indicated in green.

Table 9. In-sample estimates for different correlation forecasting models

	Short horizon (*h*=1)		Medium horizon (*h*=5)		Long horizon (*h*=20)	
	MHAR	RM-MHARX	MHAR	RM-MHARX	MHAR	RM-MHARX
θ_d	0.088	0.089	0.060	0.060	0.043	0.043
	(0.004)	(0.008)	(0.002)	(0.005)	(0.002)	(0.008)
θ_w	0.169	0.166	0.153	0.151	0.096	0.095
	(0.008)	(0.015)	(0.004)	(0.010)	(0.003)	(0.015)
θ_m	0.431	0.433	0.418	0.419	0.398	0.398
	(0.008)	(0.018)	(0.005)	(0.011)	(0.004)	(0.018)
α		0.006		0.008		0.008
		(0.004)		(0.002)		(0.002)
Adj. R^2	0.713	0.714	0.852	0.853	0.909	0.910

Note: The table reports the in-sample parameter estimates, standard errors (in parentheses) and adjusted R^2 for different models.

Table 10. Out-of-sample forecasting losses differences

	Short horizon (*h*=1)				Medium horizon (*h*=5)				Long horizon (*h*=20)			
	L^{Eucl}	L^{Frob}	L^{QLIKE}	L^{Stein}	L^{Eucl}	L^{Frob}	L^{QLIKE}	L^{Stein}	L^{Eucl}	L^{Frob}	L^{QLIKE}	L^{Stein}
Group 1:												
HAR-DRD	**0.001**	**0.002**	-0.008	-0.008	**0.006**	**0.009**	-0.002	-0.002	**0.008**	**0.012**	-0.004	-0.004
RM-HARX-DRD	**0.001**	**0.002**	-0.007	-0.007	**0.005**	**0.008**	0.001	0.001	**0.007**	**0.011**	-0.001	-0.001
PCA-RM-HARX-DRD	**0.001**	**0.001**	-0.006	-0.006	**0.004**	**0.006**	0.002	0.002	**0.007**	**0.009**	0.001	0.001
Lasso-RM-HARX-DRD	**0.001**	**0.002**	-0.007	-0.007	**0.004**	**0.007**	0.002	0.002	0.004	0.006	-0.005	-0.005
Group 2:												
HARJ-DRD	**0.001**	**0.002**	-0.006	-0.006	**0.006**	**0.009**	0.000	0.000	**0.008**	**0.012**	-0.004	-0.004
RM-HARJX-DRD	**0.000**	**0.001**	-0.005	-0.005	**0.005**	**0.008**	0.003	0.003	**0.007**	**0.010**	0.000	0.000
PCA-RM-HARJX-DRD	0.000	0.000	-0.003	-0.003	**0.004**	**0.006**	**0.004**	0.004	**0.006**	**0.009**	**0.001**	0.001
Lasso-RM-HARJX-DRD	**0.001**	**0.001**	-0.006	-0.006	**0.004**	**0.007**	0.003	0.003	0.004	0.006	-0.005	-0.005
Group 3:												
HARCJ-DRD	**0.002**	**0.004**	-0.012	-0.012	**0.008**	**0.013**	-0.006	-0.006	**0.010**	**0.016**	-0.008	-0.008
RM-HARCJX-DRD	**0.001**	**0.003**	-0.009	-0.009	**0.007**	**0.011**	-0.002	-0.002	**0.009**	**0.014**	-0.003	-0.003
PCA-RM-HARCJX-DRD	**0.001**	**0.001**	-0.007	-0.007	**0.006**	**0.009**	0.000	0.000	**0.008**	**0.012**	-0.001	-0.001
Lasso-RM-HARCJX-DRD	**0.001**	**0.003**	-0.010	-0.010	**0.006**	**0.009**	0.001	0.001	0.004	0.007	-0.003	-0.003
Group 4:												
HARRS-DRD	**0.002**	**0.003**	-0.009	-0.009	**0.006**	**0.009**	-0.002	-0.002	**0.008**	**0.012**	-0.005	-0.005
RM-HARRSX-DRD	**0.001**	**0.002**	-0.006	-0.006	**0.005**	**0.007**	0.001	0.001	**0.008**	**0.011**	-0.002	-0.002
PCA-RM-HARRSX-DRD	**0.001**	**0.001**	-0.005	-0.005	**0.004**	**0.006**	0.003	0.003	**0.007**	**0.010**	-0.001	-0.001
Lasso-RM-HARRSX-DRD	**0.001**	**0.002**	-0.007	-0.007	**0.004**	**0.007**	0.002	0.002	0.004	0.007	-0.003	-0.003

Note: This table presents the out-of-sample covariance matrix forecast loss differences. These are between the original results in Table 5 and those obtained after replacing the correlation matrix forecasting model with the RM-MHARX model, while keeping the various realized variance forecasting models unchanged. Numbers in shade denote the new losses are lower than the original. Numbers in boldface indicate that the differences are significant according to the DM test.

Appendices:

A. Descriptions on the GARCH, SV, and DCC-GARCH models employed for the extraction of relevant information from the ECI

GARCH model:

Let $y_t = ECI_t$, we use the following univariate GARCH (1,1) model to extract the volatility of ECI of a certain state,

$$y_t = \mu + \varepsilon_t, \quad \text{(A.1)}$$

$$\varepsilon_t = z_t\sigma_t, z_t \sim \text{i.i.d.} N(0,1), \quad \text{(A.2)}$$

$$\sigma_t^2 = \omega + \alpha\varepsilon_{t-1}^2 + \beta\sigma_{t-1}^2, \omega > 0, \alpha + \beta < 1. \quad \text{(A.3)}$$

The extracted volatility is σ_t.

SV model:

In Section 6, we replace the GARCH model with the SV mode to extract the volatility of ECI. Following, e.g., Jacquieretal.(1994) and Kimetal.(1998), the SV model is experessed as,

$$y_t = \exp\left(\frac{h_t}{2}\right)\epsilon_t, \quad \text{(A.4)}$$

$$h_t = \mu + \phi(h_{t-1} - \mu) + \sigma\eta_t, \quad \text{(A.5)}$$

$$\epsilon_t, \eta_t \sim \text{i.i.d.} \mathrm{N}(0,1). \quad \text{(A.6)}$$

The extracted volatility is $\sigma_t = \exp\left(\frac{h_t}{2}\right)$.

DCC-GARCH model:

In Section 7, we utilize the DCC-GARCH model to extract the dynamic correlation of ECIs. Consider the follow multivariate GARCH model,

$$\boldsymbol{y}_t = \boldsymbol{\mu} + \boldsymbol{\varepsilon}_t, \quad \text{(A.7)}$$

$$\boldsymbol{\varepsilon}_t = \boldsymbol{H}_t^{1/2}\boldsymbol{z}_t, \boldsymbol{z}_t \sim \text{i.i.d.} \mathbf{N}(0, \mathbf{I}_\mathrm{N}). \quad \text{(A.8)}$$

where $\boldsymbol{H}_t$ is an $N \times N$ latent positive definite covariance matrix of $\boldsymbol{y}_t$ and $\mathbf{I}_\mathrm{N}$ is an $N \times N$ identity matrix.

According to the Dynamic Conditional Correlation (DCC) in Engle (2002), the covariance matrix $\boldsymbol{H}_t$ can be decomposed as,

$$\boldsymbol{H}_t = \boldsymbol{D}_t \boldsymbol{R}_t \boldsymbol{D}_t = \rho_{ij}\sqrt{h_{ii,t}h_{jj,t}}, \tag{A.9}$$

$$\boldsymbol{D}_t = diag\left(\sqrt{h_{11,t}}, \dots, \sqrt{h_{nn,t}}\right), \tag{A.10}$$

$$\boldsymbol{R}_t = diag(\boldsymbol{Q}_t)^{-1/2}\boldsymbol{Q}_t diag(\boldsymbol{Q}_t)^{-1/2}, \tag{A.11}$$

$$\boldsymbol{Q}_t = (1 - a - b)\overline{\boldsymbol{Q}} + a(\boldsymbol{z}_{t-1}\boldsymbol{z}'_{t-1}) + b\boldsymbol{Q}_{t-1}, \tag{A.12}$$

$$a, b > 0, a + b < 1. \tag{A.13}$$

The extracted dynamic correlation matrix is $\boldsymbol{R}_t$.

B. The expression of all forecasting models mentioned in the paper

Table B1. Summary of realized covariance matrix forecasting models

Univariate realized variance forecasting models

Group 1:

HAR model:

$$\log(RV_{t+\frac{h}{L}}) = \beta_0 + \beta_d \log(RV_t^d) + \beta_w \log(RV_t^w) + \beta_m \log(RV_t^m) + \varepsilon_t, t = \frac{1}{L}, \frac{2}{L}, \dots, 1 + \frac{1}{L}, \dots, T - 1 + \frac{1}{L}, \dots, T.$$

RM-HARX model:

$$\log(RV_{t+\frac{l}{L}+\frac{h}{L}}) = \beta_{0,l} + \beta_{d,l} \log\left(RV^d_{t+\frac{l}{L}}\right) + \beta_{w,l} \log\left(RV^w_{t+\frac{l}{L}}\right) + \beta_{m,l} \log\left(RV^m_{t+\frac{l}{L}}\right) + \alpha_l \log(Vol_t^{ECI}) + \varepsilon_{t+\frac{l}{L}+\frac{h}{L}}, t = 0,1, \dots, T-1, l = 1,2, \dots, L.$$

PCA-HARX model:

$$\log(RV_{t+\frac{l}{L}+\frac{h}{L}}) = \beta_{0,l} + \beta_{d,l} \log\left(RV^d_{t+\frac{l}{L}}\right) + \beta_{w,l} \log\left(RV^w_{t+\frac{l}{L}}\right) + \beta_{m,l} \log\left(RV^m_{t+\frac{l}{L}}\right) + \alpha_l Factor_t + \varepsilon_{t+\frac{l}{L}+\frac{h}{L}}, t = 0,1, \dots, T-1, l = 1,2, \dots, L.$$

Lasso-RM-HARX model:

$$\log(RV_{t+\frac{l}{L}+\frac{h}{L}}) = \beta_{0,l} + \beta_{d,l} \log\left(RV^d_{t+\frac{l}{L}}\right) + \beta_{w,l} \log\left(RV^w_{t+\frac{l}{L}}\right) + \beta_{m,l} \log\left(RV^m_{t+\frac{l}{L}}\right) + \sum_{n=1}^{50} \alpha_{n,l} \log\left(Vol_{n,t}^{ECI}\right) + \varepsilon_{t+\frac{l}{L}+\frac{h}{L}}, t = 0,1, \dots, T-1, l = 1,2, \dots, L.$$

Group 2:

HARJ model:

$$\log(RV_{t+\frac{h}{L}}) = \beta_0 + \beta_d \log(RV_t^d) + \beta_w \log(RV_t^w) + \beta_m \log(RV_t^m) + \gamma_d \log(J_t + 1) + \varepsilon_t, t = \frac{1}{L}, \frac{2}{L}, \dots, 1 + \frac{1}{L}, \dots, T - 1 + \frac{1}{L}, \dots, T.$$

RM-HARJX model:

$$\log(RV_{t+\frac{l}{L}+\frac{h}{L}}) = \beta_{0,l} + \beta_{d,l} \log\left(RV^d_{t+\frac{l}{L}}\right) + \beta_{w,l} \log\left(RV^w_{t+\frac{l}{L}}\right) + \beta_{m,l} \log\left(RV^m_{t+\frac{l}{L}}\right) + \gamma_{d,l} \log(J_{t+\frac{l}{L}} + 1) + \alpha_l \log(Vol_t^{ECI}) + \varepsilon_{t+\frac{l}{L}+\frac{h}{L}}, t = 0,1, \dots, T-1, l = 1,2, \dots, L.$$

PCA-HARJX model:

$$\log(RV_{t+\frac{l}{L}+\frac{h}{L}}) = \beta_{0,l} + \beta_{d,l} \log\left(RV^d_{t+\frac{l}{L}}\right) + \beta_{w,l} \log\left(RV^w_{t+\frac{l}{L}}\right) + \beta_{m,l} \log\left(RV^m_{t+\frac{l}{L}}\right) + \gamma_{d,l} \log(J_{t+\frac{l}{L}} + 1) + \alpha_l Factor_t + \varepsilon_{t+\frac{l}{L}+\frac{h}{L}}, t = 0,1, \dots, T-1, l = 1,2, \dots, L.$$

Lasso-RM-HARJX model:

$$\log\left(RV_{t+\frac{l}{L}+\frac{h}{L}}\right) = \beta_{0,l} + \beta_{d,l}\log\left(RV^{d}_{t+\frac{l}{L}}\right) + \beta_{w,l}\log\left(RV^{w}_{t+\frac{l}{L}}\right) + \beta_{m,l}\log\left(RV^{m}_{t+\frac{l}{L}}\right) + \gamma_{d,l}\log\left(J_{t+\frac{l}{L}}+1\right) + \sum_{n=1}^{50}\alpha_{n,l}\log\left(Vol^{ECI}_{n,t}\right) + \varepsilon_{t+\frac{l}{L}+\frac{h}{L}}, t = 0,1,\ldots,T-1, l = 1,2,\ldots,L.$$

Group 3:

HARCJ model:

$$\log\left(RV_{t+\frac{h}{L}}\right) = \beta_0 + \beta_d\log\left(CV^{d}_{t}\right) + \beta_w\log\left(CV^{w}_{t}\right) + \beta_m\log\left(CV^{m}_{t}\right) + \gamma_d\log\left(CJ^{d}_{t}+1\right) + \gamma_w\log\left(CJ^{w}_{t}+1\right) + \gamma_m\log\left(CJ^{m}_{t}+1\right) + \varepsilon_t, t = \frac{1}{L},\frac{2}{L},\ldots,1+\frac{1}{L},\ldots,T-1+\frac{1}{L},\ldots,T.$$

RM-HARX model:

$$\log\left(RV_{t+\frac{l}{L}+\frac{h}{L}}\right) = \beta_{0,l} + \beta_{d,l}\log\left(CV^{d}_{t+\frac{l}{L}}\right) + \beta_{w,l}\log\left(CV^{w}_{t+\frac{l}{L}}\right) + \beta_{m,l}\log\left(CV^{m}_{t+\frac{l}{L}}\right) + \gamma_{d,l}\log\left(CJ^{d}_{t+\frac{l}{L}}+1\right) + \gamma_{w,l}\log\left(CJ^{w}_{t+\frac{l}{L}}+1\right) + \gamma_{m,l}\log\left(CJ^{m}_{t+\frac{l}{L}}+1\right) + \alpha_l\log\left(Vol^{ECI}_{t}\right) + \varepsilon_{t+\frac{l}{L}+\frac{h}{L}}, t = 0,1,\ldots,T-1, l = 1,2,\ldots,L.$$

PCA-HARX model:

$$\log\left(RV_{t+\frac{l}{L}+\frac{h}{L}}\right) = \beta_{0,l} + \beta_{d,l}\log\left(CV^{d}_{t+\frac{l}{L}}\right) + \beta_{w,l}\log\left(CV^{w}_{t+\frac{l}{L}}\right) + \beta_{m,l}\log\left(CV^{m}_{t+\frac{l}{L}}\right) + \gamma_{d,l}\log\left(CJ^{d}_{t+\frac{l}{L}}+1\right) + \gamma_{w,l}\log\left(CJ^{w}_{t+\frac{l}{L}}+1\right) + \gamma_{m,l}\log\left(CJ^{m}_{t+\frac{l}{L}}+1\right) + \alpha_l Factor_t + \varepsilon_{t+\frac{l}{L}+\frac{h}{L}}, t = 0,1,\ldots,T-1, l = 1,2,\ldots,L.$$

Lasso-RM-HARX model:

$$\log\left(RV_{t+\frac{l}{L}+\frac{h}{L}}\right) = \beta_{0,l} + \beta_{d,l}\log\left(CV^{d}_{t+\frac{l}{L}}\right) + \beta_{w,l}\log\left(CV^{w}_{t+\frac{l}{L}}\right) + \beta_{m,l}\log\left(CV^{m}_{t+\frac{l}{L}}\right) + \gamma_{d,l}\log\left(CJ^{d}_{t+\frac{l}{L}}+1\right) + \gamma_{w,l}\log\left(CJ^{w}_{t+\frac{l}{L}}+1\right) + \gamma_{m,l}\log\left(CJ^{m}_{t+\frac{l}{L}}+1\right) + \sum_{n=1}^{50}\alpha_{n,l}\log\left(Vol^{ECI}_{n,t}\right) + \varepsilon_{t+\frac{l}{L}+\frac{h}{L}}, t = 0,1,\ldots,T-1, l = 1,2,\ldots,L.$$

Group 4:

HARRS model:

$$\log(RV_{t+\frac{h}{L}}) = \beta_0 + \beta_{d,l}\log(PSV^{d}_{t+\frac{l}{L}}) + \beta_{w,l}\log(PSV^{w}_{t+\frac{l}{L}}) + \beta_{m,l}\log(PSV^{m}_{t+\frac{l}{L}}) + \gamma_{d,l}\log(NSV^{d}_{t+\frac{l}{L}}) + \gamma_{w,l}\log(NSV^{w}_{t+\frac{l}{L}}) + \gamma_{m,l}\log(NSV^{m}_{t+\frac{l}{L}}) + \varepsilon_t, t = \frac{1}{L}, \frac{2}{L}, \ldots, 1 + \frac{1}{L}, \ldots, T - 1 + \frac{1}{L}, \ldots, T.$$

RM-HARRSX model:

$$\log(RV_{t+\frac{l}{L}+\frac{h}{L}}) = \beta_{0,l} + \beta_{d,l}\log(PSV^{d}_{t+\frac{l}{L}}) + \beta_{w,l}\log(PSV^{w}_{t+\frac{l}{L}}) + \beta_{m,l}\log(PSV^{m}_{t+\frac{l}{L}}) + \gamma_{d,l}\log(NSV^{d}_{t+\frac{l}{L}}) + \gamma_{w,l}\log(NSV^{w}_{t+\frac{l}{L}}) + \gamma_{m,l}\log(NSV^{m}_{t+\frac{l}{L}}) + \alpha_l \log(Vol^{ECI}_t) + \varepsilon_{t+\frac{l}{L}+\frac{h}{L}}, t = 0,1, \ldots, T-1, l = 1,2, \ldots, L.$$

PCA-HARRSX model:

$$\log(RV_{t+\frac{l}{L}+\frac{h}{L}}) = \beta_{0,l} + \beta_{d,l}\log(PSV^{d}_{t+\frac{l}{L}}) + \beta_{w,l}\log(PSV^{w}_{t+\frac{l}{L}}) + \beta_{m,l}\log(PSV^{m}_{t+\frac{l}{L}}) + \gamma_{d,l}\log(NSV^{d}_{t+\frac{l}{L}}) + \gamma_{w,l}\log(NSV^{w}_{t+\frac{l}{L}}) + \gamma_{m,l}\log(NSV^{m}_{t+\frac{l}{L}}) + \alpha_l Factor_t + \varepsilon_{t+\frac{l}{L}+\frac{h}{L}}, t = 0,1, \ldots, T-1, l = 1,2, \ldots, L.$$

Lasso-RM-HARRSX model:

$$\log(RV_{t+\frac{l}{L}+\frac{h}{L}}) = \beta_{0,l} + \beta_{d,l}\log(PSV^{d}_{t+\frac{l}{L}}) + \beta_{w,l}\log(PSV^{w}_{t+\frac{l}{L}}) + \beta_{m,l}\log(PSV^{m}_{t+\frac{l}{L}}) + \gamma_{d,l}\log(NSV^{d}_{t+\frac{l}{L}}) + \gamma_{w,l}\log(NSV^{w}_{t+\frac{l}{L}}) + \gamma_{m,l}\log(NSV^{m}_{t+\frac{l}{L}}) + \sum_{n=1}^{50} \alpha_{n,l} \log(Vol^{ECI}_{n,t}) + \varepsilon_{t+\frac{l}{L}+\frac{h}{L}}, t = 0,1, \ldots, T-1, l = 1,2, \ldots, L.$$

Relaized correlation matrix forecasting models

Scalar MHAR model:

$$vech(\boldsymbol{A}_{t+h}) = \boldsymbol{c} + \theta_d vech(\boldsymbol{A}^{d}_t) + \theta_w vech(\boldsymbol{A}^{w}_t) + \theta_m vech(\boldsymbol{A}^{m}_t) + \boldsymbol{\epsilon}_{t+h}, t = \frac{1}{L}, \frac{2}{L}, \ldots, 1 + \frac{1}{L}, \ldots, T - 1 + \frac{1}{L}, \ldots, T.$$

Scalar RM-MHARX model:

$$vech(\boldsymbol{A}_{t+\frac{l}{L}+\frac{h}{L}}) = \boldsymbol{c}_l + \theta_{d,l} vech(\boldsymbol{A}^{d}_{t+\frac{l}{L}}) + \theta_{w,l} vech(\boldsymbol{A}^{w}_{t+\frac{l}{L}}) + \theta_{m,l} vech(\boldsymbol{A}^{m}_{t+\frac{l}{L}+\frac{h}{L}}) + \alpha_l vech(\boldsymbol{CX}_t) + \boldsymbol{\epsilon}_{t+\frac{l}{L}+\frac{h}{L}}, t = 0,1, \ldots, T-1, l = 1,2, \ldots, L,$$

C. Tables

Table C1. The chosen US states for different dimension scenarios

State	N=10	N=20	N=30	N=40	N=50	State	N=10	N=20	N=30	N=40	N=50
Alabama					△	Montana	△	△	△	△	△
Alaska					△	Nebraska		△	△	△	△
Arizona	△	△	△	△	△	Nevada		△	△	△	△
Arkansas			△	△	△	New Hampshire		△	△	△	△
California		△	△	△	△	New Jersey				△	△
Colorado					△	New Mexico	△	△	△	△	△
Connecticut		△	△	△	△	New York			△	△	△
Delaware		△	△	△	△	North Carolina				△	△
Florida		△	△	△	△	North Dakota					△
Georgia		△	△	△	△	Ohio					△
Hawaii			△	△	△	Oklahoma			△	△	△
Idaho			△	△	△	Oregon	△	△	△	△	△
Illinois				△	△	Pennsylvania					△
Indiana	△	△	△	△	△	Rhode Island				△	△
Iowa	△	△	△	△	△	South Carolina		△	△	△	△
Kansas					△	South Dakota		△	△	△	△
Kentucky			△	△	△	Tennessee	△	△	△	△	△
Louisiana				△	△	Texas	△	△	△	△	△
Maine			△	△	△	Utah					△
Maryland				△	△	Vermont			△	△	△
Massachusetts			△	△	△	Virginia				△	△
Michigan				△	△	Washington					△
Minnesota					△	West Virginia	△	△	△	△	△
Mississippi	△	△		△	△	Wisconsin			△	△	△
Missouri			△	△	△	Wyoming				△	△

Note: These states are selected randomly through the following process in R software: First, the "set.seed(123)" function is used to set the seed for reproducibility. Then, corresponding numbers are randomly sampled from the range of 1 to 50 using the "sample( )" function. Each sampled number is mapped to a specific state, resulting in the selection of states, denoted by "△".

Table C2. Out-of-sample forecasting losses (MRK)

	Short horizon (*h*=1)				Medium horizon (*h*=5)				Long horizon (*h*=20)			
	L^{Eucl}	L^{Frob}	L^{QLIKE}	L^{Stein}	L^{Eucl}	L^{Frob}	L^{QLIKE}	L^{Stein}	L^{Eucl}	L^{Frob}	L^{QLIKE}	L^{Stein}
Group 1:												
HAR-DRD	5.754	**7.150**	**31.160**	**41.918**	4.128	5.016	**5.703**	**2.590**	3.649	4.425	**5.851**	**1.435**
RM-HARX-DRD	**5.735***	**7.125***	31.379	42.137	**4.110***	4.992*	**5.707**	**2.594**	**3.628***	**4.396***	**5.863**	**1.447**
PCA-RM-HARX-DRD	**5.724***	**7.114***	**31.196**	**41.955**	**4.110***	**4.989***	**5.698***	**2.584***	**3.643***	**4.406***	**5.863**	**1.447**
Lasso-RM-HARX-DRD	5.763	7.159	31.534	42.293	4.217	5.113	5.954	2.840	5.394	6.375	7.217	2.801
Group 2:												
HARJ-DRD	5.773	7.182	**30.957**	**41.716**	4.129	5.021	5.714	2.601	**3.599**	**4.383**	**5.856**	**1.440**
RM-HARJX-DRD	5.755*	7.157*	**31.204**	**41.962**	**4.105***	4.991*	5.720	2.606	**3.566***	**4.348***	**5.864**	**1.448**
PCA-RM-HARJX-DRD	**5.749***	**7.149***	**30.994**	**41.753**	**4.099***	**4.981***	**5.705***	**2.591***	**3.572***	**4.347***	**5.861**	**1.445**
Lasso-RM-HARJX-DRD	5.788	7.195	31.310	42.069	4.217	5.113	5.971	2.858	5.383	6.362	7.238	2.822
Group 3:												
HARCJ-DRD	5.849	7.231	31.820	42.578	4.220	5.091	5.726	2.612	3.720	4.491	5.886	1.470
RM-HARCJX-DRD	5.842	7.220*	31.726*	42.484*	4.201*	5.077*	**5.710***	**2.597***	3.681*	4.464*	5.877*	1.461*
PCA-RM-HARCJX-DRD	5.803*	7.184*	**31.065***	**41.824***	4.152*	5.029*	**5.662***	**2.549***	**3.624***	**4.405***	**5.839***	**1.423***
Lasso-RM-HARCJX-DRD	5.836*	7.219*	31.543*	42.301*	4.191*	5.071*	5.848	2.735	5.196	6.130	7.157	2.741
Group 4:												
HARRS-DRD	**5.732**	**7.100**	32.413	43.172	**4.076**	**4.956**	5.728	2.615	**3.575**	**4.351**	5.899	1.483
RM-HARRSX-DRD	**5.714***	**7.078***	32.549	43.308	**4.064***	**4.942***	5.724*	2.611*	**3.573***	**4.349***	5.907	1.491
PCA-RM-HARRSX-DRD	**5.684***	**7.050***	32.113*	42.872*	**4.057***	**4.932***	**5.708***	**2.595***	**3.595**	**4.364**	5.904	1.488
Lasso-RM-HARRSX-DRD	**5.727***	**7.101**	32.360*	43.119*	4.164	5.048	5.892	2.779	5.184	6.133	7.138	2.723

Note: The table reports out-of-sample forecast loss for the five groups of models. Entries in boldface indicate models that are part of the 75% model confidence set (MCS) for all models across the relevant loss. For each group, RM models that significantly improve on their non-RM benchmark model via DM test are indicated by an asterisk.

Table C3. Out-of-sample forecasting losses (*N*=20)

	Short horizon (*h*=1)				Medium horizon (*h*=5)				Long horizon (*h*=20)			
	L^{Eucl}	L^{Frob}	L^{QLIKE}	L^{Stein}	L^{Eucl}	L^{Frob}	L^{QLIKE}	L^{Stein}	L^{Eucl}	L^{Frob}	L^{QLIKE}	L^{Stein}
Group 1:												
HAR-DRD	**7.027**	**9.078**	5.003	9.383	**5.620**	7.206	**4.844**	**3.889**	**5.390**	**6.911**	**5.318**	**2.470**
RM-HARX-DRD	**7.032**	**9.085**	**4.988***	**9.369***	**5.598***	**7.179***	**4.827***	**3.872***	**5.367***	**6.888***	**5.308***	**2.460**
PCA-RM-HARX-DRD	**7.014***	**9.063***	**4.984***	**9.365***	**5.590***	**7.163***	**4.809***	**3.855***	**5.383***	**6.889***	**5.290***	**2.442***
Lasso-RM-HARX-DRD	7.051	9.106	5.113	9.493	5.815	7.447	5.179	4.225	8.675	10.759	8.815	5.967
Group 2:												
HARJ-DRD	**7.010**	**9.054**	5.018	9.399	5.657	7.255	4.901	3.947	**5.391**	**6.928**	5.360	2.512
RM-HARJX-DRD	**7.007**	**9.051***	5.000*	**9.380***	**5.619***	7.207*	4.882*	3.927*	**5.353***	**6.896***	**5.348***	**2.500***
PCA-RM-HARJX-DRD	**6.996***	**9.036***	**4.993***	**9.373***	**5.597***	**7.173***	**4.858***	**3.904***	**5.352***	**6.872***	**5.325***	**2.477***
Lasso-RM-HARJX-DRD	**7.032**	**9.080**	5.145	9.525	5.797	7.422	5.169	4.215	8.618	10.694	8.778	5.930
Group 3:												
HARCJ-DRD	7.117	9.161	4.996	**9.376**	5.767	7.363	4.908	3.954	5.490	7.029	5.427	2.579
RM-HARCJX-DRD	7.117	9.164	**4.964***	**9.344***	5.740*	7.338*	4.881*	3.926*	5.456*	7.018*	5.407*	2.559*
PCA-RM-HARCJX-DRD	7.096*	9.140*	**4.926***	**9.306***	5.701*	7.288*	**4.837***	**3.883***	**5.409***	**6.946***	**5.357***	**2.509***
Lasso-RM-HARCJX-DRD	7.122	9.167	5.082	9.462	5.780	7.375	5.064	4.110	8.457	10.512	8.858	6.010
Group 4:												
HARRS-DRD	7.048	9.097	5.010	9.391	5.647	7.236	4.869	3.915	5.424	**6.939**	5.435	2.587
RM-HARRSX-DRD	7.049	9.098	**4.989***	**9.370***	**5.618***	**7.199***	**4.847***	3.893*	**5.402***	**6.916***	5.419*	2.572*
PCA-RM-HARRSX-DRD	**7.031***	**9.077***	**4.984***	**9.364***	**5.609***	**7.183***	**4.827***	**3.873***	**5.413***	**6.911***	5.391*	2.543*
Lasso-RM-HARRSX-DRD	7.065	9.115	5.101	9.481	5.752	7.355	5.095	4.141	8.564	10.632	8.634	5.786

Note: The table reports out-of-sample forecast loss for the five groups of models. Entries in boldface indicate models that are part of the 75% model confidence set (MCS) for all models across the relevant loss. For each group, RM models that significantly improve on their non-RM benchmark model via DM test are indicated by an asterisk.

Table C4. Out-of-sample forecasting losses (N=30)

	Short horizon (h=1)				Medium horizon (h=5)				Long horizon (h=20)			
	L^{Eucl}	L^{Frob}	L^{QLIKE}	L^{Stein}	L^{Eucl}	L^{Frob}	L^{QLIKE}	L^{Stein}	L^{Eucl}	L^{Frob}	L^{QLIKE}	L^{Stein}
Group 1:												
HAR-DRD	**9.990**	**13.128**	7.010	19.383	7.838	10.256	**5.832**	**7.344**	**7.414**	9.734	**6.377**	**4.353**
RM-HARX-DRD	**9.996**	**13.138**	6.978*	**19.352***	**7.815***	**10.225***	**5.807***	**7.319***	**7.399***	**9.712***	**6.391**	**4.367**
PCA-RM-HARX-DRD	**9.973***	**13.110***	6.981*	19.355*	**7.804***	**10.208***	**5.784***	**7.296***	**7.417**	**9.719***	**6.370***	**4.346***
Lasso-RM-HARX-DRD	10.029	13.173	7.295	19.669	7.995	10.431	6.299	7.811	10.197	12.793	9.901	7.877
Group 2:												
HARJ-DRD	**9.956**	**13.087**	6.976	**19.350**	7.869	10.301	5.911	7.423	7.420	9.759	6.416	4.392
RM-HARJX-DRD	**9.953**	**13.084**	**6.948***	**19.322***	**7.824***	**10.242***	5.885*	7.396*	**7.392***	9.731*	6.423	4.399
PCA-RM-HARJX-DRD	**9.939***	**13.066***	**6.929***	**19.303***	**7.801***	**10.209***	**5.854***	**7.366***	**7.394***	**9.714***	**6.400***	**4.376***
Lasso-RM-HARJX-DRD	10.021	13.164	7.276	19.649	7.922	10.352	6.115	7.627	9.061	11.712	8.482	6.458
Group 3:												
HARCJ-DRD	10.086	13.226	**6.882**	**19.256**	7.959	10.386	5.864	7.376	7.498	9.845	6.448	4.424
RM-HARCJX-DRD	10.088	13.229	**6.816***	**19.190***	7.941*	10.368*	**5.825***	**7.337***	7.488	9.850	6.455	4.431
PCA-RM-HARCJX-DRD	10.065*	13.203*	**6.754***	**19.128***	7.902*	10.317*	**5.769***	**7.281***	7.447*	9.787*	**6.397***	**4.373***
Lasso-RM-HARCJX-DRD	10.080	13.211	7.192	19.565	7.955	10.351	6.139	7.651	10.456	13.130	10.512	8.488
Group 4:												
HARRS-DRD	10.017	13.159	6.986	19.360	7.858	10.278	5.851	**7.363**	7.435	9.747	6.499	4.475
RM-HARRSX-DRD	10.017	13.159	**6.948***	**19.322***	**7.826***	**10.235***	**5.824***	**7.336***	**7.415***	**9.718***	6.500	4.476
PCA-RM-HARRSX-DRD	**9.993***	**13.131***	**6.934***	**19.308***	**7.814***	**10.217***	**5.794***	**7.306***	7.427*	**9.718***	6.474*	4.449*
Lasso-RM-HARRSX-DRD	10.029	13.169	7.180	19.554	7.899	10.313	6.118	7.630	9.424	12.009	10.190	8.166

Note: The table reports out-of-sample forecast loss for the five groups of models. Entries in boldface indicate models that are part of the 75% model confidence set (MCS) for all models across the relevant loss. For each group, RM models that significantly improve on their non-RM benchmark model via DM test are indicated by an asterisk.

Table C5. Out-of-sample forecasting losses (*N*=40)

	Short horizon (*h*=1)				Medium horizon (*h*=5)				Long horizon (*h*=20)			
	L^{Eucl}	L^{Frob}	L^{QLIKE}	L^{Stein}	L^{Eucl}	L^{Frob}	L^{QLIKE}	L^{Stein}	L^{Eucl}	L^{Frob}	L^{QLIKE}	L^{Stein}
Group 1:												
HAR-DRD	**26.224**	**30.162**	7.558	34.399	21.758	24.721	**3.883**	**12.078**	18.951	21.662	**4.308**	**6.649**
RM-HARX-DRD	**26.253**	**30.193**	**7.494***	**34.335***	**21.749***	**24.703***	**3.846***	**12.041***	**18.869***	**21.571***	**4.340**	**6.681**
PCA-RM-HARX-DRD	**26.236**	**30.172**	**7.497***	**34.338***	**21.669***	**24.623***	**3.814***	**12.009***	**18.741***	**21.451***	**4.290***	**6.631***
Lasso-RM-HARX-DRD	26.467	30.407	7.934	34.775	22.094	25.140	4.782	12.977	27.629	30.797	11.324	13.665
Group 2:												
HARJ-DRD	**26.179**	**30.107**	**7.435**	**34.276**	21.761	24.736	3.979	12.174	18.992	21.732	**4.356**	**6.697**
RM-HARJX-DRD	**26.248**	**30.175**	**7.391***	**34.231***	**21.745***	**24.706***	**3.948***	**12.143***	**18.886***	**21.624***	**4.386**	**6.726**
PCA-RM-HARJX-DRD	**26.200**	**30.126**	**7.356***	**34.197***	**21.671***	**24.627***	**3.907***	**12.102***	**18.758***	**21.489***	**4.335***	**6.676***
Lasso-RM-HARJX-DRD	26.357	30.306	7.835	34.676	21.972	24.991	4.401	12.596	24.645	27.861	10.385	12.726
Group 3:												
HARCJ-DRD	26.487	30.422	**7.426**	**34.254**	22.433	25.398	3.996	**12.140**	19.188	21.938	4.423	6.745
RM-HARCJX-DRD	26.575	30.506	**7.288***	**34.116***	22.482	25.442	3.957*	**12.102***	19.209	21.964	4.470	6.793
PCA-RM-HARCJX-DRD	26.516	30.450	**7.119***	**33.948***	22.325*	25.277*	**3.868***	**12.013***	19.031*	21.775*	**4.390***	**6.712***
Lasso-RM-HARCJX-DRD	27.169	31.061	7.880	34.709	24.307	27.240	5.838	13.986	33.266	36.371	12.730	15.071
Group 4:												
HARRS-DRD	26.758	30.673	7.691	34.537	22.342	25.282	4.025	12.223	19.786	22.469	4.651	6.987
RM-HARRSX-DRD	26.860	30.771	7.596*	34.441*	22.364	25.290	3.983*	12.181*	19.780	22.449*	4.665	7.000
PCA-RM-HARRSX-DRD	26.731*	30.643*	7.553*	34.399*	22.224*	25.152*	**3.927***	**12.125***	19.519*	22.197*	4.588*	6.924*
Lasso-RM-HARRSX-DRD	27.395	31.299	7.931	34.777	23.402	26.380	4.701	12.899	28.322	31.443	11.404	13.745

Note: The table reports out-of-sample forecast loss for the five groups of models. Entries in boldface indicate models that are part of the 75% model confidence set (MCS) for all models across the relevant loss. For each group, RM models that significantly improve on their non-RM benchmark model via DM test are indicated by an asterisk.

Table C6. Out-of-sample forecasting losses (*N*=50)

	Short horizon (*h*=1)				Medium horizon (*h*=5)				Long horizon (*h*=20)			
	L^{Eucl}	L^{Frob}	L^{QLIKE}	L^{Stein}	L^{Eucl}	L^{Frob}	L^{QLIKE}	L^{Stein}	L^{Eucl}	L^{Frob}	L^{QLIKE}	L^{Stein}
Group 1:												
HAR-DRD	**30.660**	**35.645**	12.517	53.507	**24.760**	**28.516**	**4.558**	**16.915**	**21.616**	25.069	**5.318**	**9.410**
RM-HARX-DRD	**30.677**	**35.661**	**12.444***	**53.434***	**24.722***	**28.468***	**4.486***	**16.843***	**21.522***	**24.964***	**5.289***	**9.381***
PCA-RM-HARX-DRD	**30.703**	**35.678**	**12.452***	**53.442***	**24.665***	**28.408***	**4.471***	**16.828***	**21.378***	**24.830***	**5.213***	**9.305***
Lasso-RM-HARX-DRD	**30.823**	**35.816**	12.914	53.904	24.979	28.860	5.512	17.868	35.085	39.521	16.006	20.097
Group 2:												
HARJ-DRD	**30.774**	**35.753**	**12.361**	**53.351**	24.817	**28.587**	4.650	17.007	**21.680**	25.162	5.372	**9.464**
RM-HARJX-DRD	**30.810**	**35.787**	**12.319***	**53.309***	**24.769***	**28.525***	**4.585***	**16.942***	**21.553***	**25.031***	**5.338***	**9.430***
PCA-RM-HARJX-DRD	**30.802**	**35.771**	**12.277***	**53.268***	**24.720***	**28.466***	**4.563***	**16.920***	**21.420***	**24.890***	**5.262***	**9.353***
Lasso-RM-HARJX-DRD	30.989	**35.980**	12.826	53.816	25.043	28.909	5.550	17.906	35.104	39.545	16.146	20.238
Group 3:												
HARCJ-DRD	31.216	36.227	12.914	53.912	25.666	29.440	5.716	18.007	21.847	25.360	5.550	9.622
RM-HARCJX-DRD	31.296	36.305	12.665*	53.663*	25.679	29.449	5.730	18.021	21.782*	25.303*	5.531*	9.603*
PCA-RM-HARCJX-DRD	31.260	36.274	**12.388***	**53.387***	25.553*	29.319*	5.489*	17.780*	**21.648***	25.160*	5.405*	**9.477***
Lasso-RM-HARCJX-DRD	31.789	36.808	15.545	56.536	27.321	31.100	6.499	18.790	36.751	41.093	18.273	22.364
Group 4:												
HARRS-DRD	31.387	36.365	13.093	54.091	25.724	29.464	4.906	17.267	22.468	25.904	5.817	9.903
RM-HARRSX-DRD	31.469	36.446	12.913*	53.911*	25.720	29.449*	4.807*	17.169*	22.388*	25.813*	5.764*	9.850*
PCA-RM-HARRSX-DRD	31.375*	36.351*	12.876*	53.874*	25.573*	29.302*	4.770*	17.131*	22.140*	25.579*	5.659*	9.745*
Lasso-RM-HARRSX-DRD	31.746	36.742	13.616	54.614	26.740	30.539	5.922	18.284	35.600	39.933	16.141	20.232

Note: The table reports out-of-sample forecast loss for the five groups of models. Entries in boldface indicate models that are part of the 75% model confidence set (MCS) for all models across the relevant loss. For each group, RM models that significantly improve on their non-RM benchmark model via DM test are indicated by an asterisk.

Table C7. Out-of-sample forecasting losses (Stochastic volatility)

	Short horizon (h=1)				Medium horizon (h=5)				Long horizon (h=20)			
	L^{Eucl}	L^{Frob}	L^{QLIKE}	L^{Stein}	L^{Eucl}	L^{Frob}	L^{QLIKE}	L^{Stein}	L^{Eucl}	L^{Frob}	L^{QLIKE}	L^{Stein}
Group 1:												
HAR-DRD	**4.432**	**5.373**	5.782	3.284	**3.624**	**4.324**	**5.850**	**1.583**	**3.503**	**4.167**	**6.119**	**1.088**
RM-HARX-DRD	**4.427***	**5.369***	**5.770***	**3.272***	**3.616***	**4.311***	**5.850**	**1.582***	**3.501***	**4.153***	**6.140**	**1.109**
PCA-RM-HARX-DRD	**4.431**	**5.371***	**5.776***	**3.278***	**3.622***	**4.313***	**5.861**	**1.594**	3.560	**4.205**	**6.182**	**1.150**
Lasso-RM-HARX-DRD	4.482	5.428	5.918	3.420	4.471	5.280	6.815	2.548	12.986	14.882	17.125	12.094
Group 2:												
HARJ-DRD	**4.417**	**5.352**	**5.776**	**3.278**	3.637	4.344	**5.867**	**1.600**	**3.463**	**4.140**	**6.127**	**1.095**
RM-HARJX-DRD	**4.405***	**5.339***	**5.767***	**3.268***	**3.603***	**4.302***	**5.865***	**1.597***	**3.413***	**4.081***	**6.123***	**1.091***
PCA-RM-HARJX-DRD	**4.410***	**5.343***	**5.767***	**3.269***	**3.605***	**4.298***	5.871	1.604	**3.476**	**4.134***	**6.177**	**1.145**
Lasso-RM-HARJX-DRD	4.481	5.422	5.903	3.405	4.435	5.231	6.797	2.529	12.623	14.512	17.000	11.968
Group 3:												
HARCJ-DRD	4.533	5.463	5.799	3.301	3.750	4.452	5.887	1.620	3.559	4.232	**6.163**	**1.131**
RM-HARCJX-DRD	4.515*	5.443*	5.780*	**3.281***	3.697*	4.396*	**5.867***	**1.600***	**3.435***	**4.105***	**6.149***	**1.117***
PCA-RM-HARCJX-DRD	4.507*	5.435*	**5.765***	**3.267***	3.705*	4.398*	**5.867***	**1.600***	**3.514***	**4.171***	**6.171**	**1.140**
Lasso-RM-HARCJX-DRD	4.560	5.490	5.866	3.368	4.300	5.054	6.615	2.348	12.444	14.144	17.053	12.021
Group 4:												
HARRS-DRD	4.456	5.394	5.793	3.295	3.644	4.345	**5.854**	**1.587**	3.530	**4.189**	**6.149**	**1.117**
RM-HARRSX-DRD	4.450*	5.387*	**5.775***	**3.277***	**3.631***	**4.325***	**5.849***	**1.582***	**3.514***	**4.158***	**6.148**	**1.115***
PCA-RM-HARRSX-DRD	4.452*	5.387*	5.782*	3.284*	3.636*	**4.327***	**5.859**	**1.592**	3.574	4.212	6.189	**1.158**
Lasso-RM-HARRSX-DRD	4.499	5.439	5.870	3.372	4.359	5.138	6.633	2.366	13.546	15.494	16.852	11.820

Note: The table reports out-of-sample forecast loss for the five groups of models. Entries in boldface indicate models that are part of the 75% model confidence set (MCS) for all models across the relevant loss. For each group, RM models that significantly improve on their non-RM benchmark model via DM test are indicated by an asterisk.

Table C8. Out-of-sample forecasting losses (alternative out-of-sample period)

	Short horizon (h=1)				Medium horizon (h=5)				Long horizon (h=20)			
	L^{Eucl}	L^{Frob}	L^{QLIKE}	L^{Stein}	L^{Eucl}	L^{Frob}	L^{QLIKE}	L^{Stein}	L^{Eucl}	L^{Frob}	L^{QLIKE}	L^{Stein}
Group 1:												
HAR-DRD	**13.875**	**15.007**	**7.673**	5.692	11.331	12.285	8.059	3.702	10.826	11.870	9.044	3.616
RM-HARX-DRD	**13.902**	**15.037**	**7.643***	**5.662***	**11.308***	**12.257***	**7.988***	**3.630***	**10.763***	**11.770***	**9.037***	**3.609***
PCA-RM-HARX-DRD	**13.994**	**15.139**	**7.652***	**5.670***	**11.268***	**12.180***	**7.954***	**3.596***	10.955	11.888	9.139	3.711
Lasso-RM-HARX-DRD	**13.938**	**15.072**	7.705	5.724	11.657	12.584	8.332	3.975	14.072	15.015	18.202	12.774
Group 2:												
HARJ-DRD	**14.042**	**15.195**	7.744	5.762	11.445	12.426	8.075	3.717	**10.754**	11.819	9.264	3.836
RM-HARJX-DRD	**14.052**	**15.207**	**7.701***	5.720*	11.405*	12.373*	7.995*	**3.637***	**10.670***	**11.698***	9.260*	3.832*
PCA-RM-HARJX-DRD	**14.152**	**15.309**	**7.670***	**5.689***	**11.301***	**12.203***	**7.921***	**3.563***	10.984	11.955	9.396	3.968
Lasso-RM-HARJX-DRD	**14.033***	**15.176***	7.777	5.796	11.558	12.486	8.326	3.968	13.949	14.915	22.764	17.336
Group 3:												
HARCJ-DRD	**15.154**	16.233	16.326	14.345	12.504	13.345	8.596	4.238	11.144	12.132	9.212	3.784
RM-HARCJX-DRD	15.199	16.284	15.650*	13.668*	12.447*	13.298*	8.566*	4.208*	11.079*	12.062*	9.193*	3.766*
PCA-RM-HARCJX-DRD	15.221	16.333	16.104*	14.122*	12.634	13.491	8.497*	4.139*	12.257	13.367	9.334	3.906
Lasso-RM-HARCJX-DRD	15.483	16.570	16.266*	14.285*	12.656	13.513	8.788	4.431	14.059	15.047	18.879	13.451
Group 4:												
HARRS-DRD	**13.700**	**14.836**	**7.612**	**5.631**	**11.270**	**12.198**	**7.818**	**3.461**	**10.442**	**11.419**	**8.695**	**3.267**
RM-HARRSX-DRD	**13.707**	**14.839**	**7.509***	**5.527***	**11.219***	**12.135***	**7.678***	**3.321***	**10.437***	**11.388***	**8.477***	**3.049***
PCA-RM-HARRSX-DRD	**13.790**	**14.928**	**7.501***	**5.520***	**11.204***	**12.082***	**7.661***	**3.303***	**10.455**	**11.357***	**8.545***	**3.117***
Lasso-RM-HARRSX-DRD	**13.868**	**15.007**	7.854	5.873	11.743	12.620	8.050	3.693	13.949	14.863	14.729	9.301

Note: The table reports out-of-sample forecast loss for the five groups of models. Entries in boldface indicate models that are part of the 75% model confidence set (MCS) for all models across the relevant loss. For each group, RM models that significantly improve on their non-RM benchmark model via DM test are indicated by an asterisk.